THE STAR FORMATION HISTORIES OF GALAXIES IN DISTANT CLUSTERS[1]

BIANCA M. POGGIANTI,[2,3,4] IAN SMAIL,[5] ALAN DRESSLER,[6] WARRICK J. COUCH,[7] AMY J. BARGER,[8] HARVEY BUTCHER,[9] RICHARD S. ELLIS,[2] AND AUGUSTUS OEMLER, JR.[6]

ABSTRACT

We present a detailed analysis of the spectroscopic catalog of galaxies in 10 distant clusters from Dressler et al. We investigate the nature of the different spectral classes defined by Dressler et al., including star-forming, poststarburst, and passive galaxy populations, and reproduce their basic properties using our spectral synthesis model. We attempt to identify the evolutionary pathways between the various spectral classes in order to search for the progenitors of the numerous poststarburst galaxies. The comparison of the spectra of the distant galaxy populations with samples drawn from the local universe leads us to identify a significant population of dust-enshrouded starburst galaxies, showing both strong Balmer absorption and relatively modest [O II] emission, that we believe are the most likely progenitors of the poststarburst population. We present the differences between the field and cluster galaxies at $z = 0.4$–0.5. We then compare the spectral and morphological properties of the distant cluster galaxies, exploring the connection between the quenching of star formation inferred from the spectra and the strong evolution of the S0 population discussed by Dressler et al. We conclude that either two different timescales and/or two different physical processes are responsible for the spectral and morphological transformation.

Subject headings: galaxies: clusters: general — galaxies: evolution — galaxies: fundamental parameters — galaxies: stellar content

1. INTRODUCTION

Of all the environments explored locally, the dense, concentrated cores of rich clusters are highly conspicuous for their lack of star-forming galaxies. Thus it came as a surprise when Butcher & Oemler (1978; see also Butcher & Oemler 1984) discovered a population of blue, possibly star-forming, galaxies in the cores of rich clusters at $z \gtrsim 0.2$. Subsequent low- and intermediate-resolution spectroscopy of these galaxies has confirmed that they are cluster members and also that star formation is the cause of their blue colors (Dressler & Gunn 1982, 1983, 1992; Lavery & Henry 1986, 1988; Couch & Sharples 1987, hereafter CS87; Henry & Lavery 1987; Soucail et al. 1988; Fabricant, McClintock, & Bautz 1991; Fabricant, Bautz, & McClintock 1994; Couch et al. 1994, 1998; Abraham et al. 1996; Fisher et al. 1998).

While the variation in the blue population within rich clusters shows evidence for dramatic evolutionary effects, additional signs of change were also uncovered by the spectroscopic studies. These included a class of galaxies, first identified by Dressler & Gunn (1983), with no detectable emission lines (and hence little or no ongoing star formation) but very strong Balmer absorption. Dressler & Gunn inferred the presence of a substantial population of A stars and concluded that an epoch of strong star formation had abruptly ended in the recent past, leaving the galaxy in a so-called poststarburst phase. In 1987 Couch & Sharples made the first attempt to synthesize a coherent view of the star formation histories of these and the other spectral populations within the clusters, hoping to identify a single evolutionary cycle through a starburst phase to the poststarburst galaxies and from there into the large population of passive galaxies seen in the clusters (see also Barger et al. 1996). However, the nature of the physical process(es) responsible for triggering and terminating the episodes of star formation in the distant clusters (and the lack of such activity today) has remained elusive.

The next major step came from high-resolution imaging with the *Hubble Space Telescope* (*HST*). Using pre- and postrefurbishment imaging, the populations of star-forming and poststarburst galaxies were morphologically identified with disk-dominated systems, a fraction of which are interacting or obviously disturbed (Couch et al. 1994, 1998; Dressler et al. 1994; Oemler, Dressler, & Butcher 1997). This supported the suggestion of galaxy-galaxy interactions as one triggering mechanism for the star formation seen in the distant clusters (Lavery & Henry 1988). However, the expectation that the high-speed encounters within clusters would be ineffective at disturbing galaxies has led to other dynamical mechanisms being suggested, including tidal disruption (Byrd & Valtonen 1990) and repeated high-speed encounters in the cluster potential ("harassment"; Moore et al. 1996; Moore, Lake, & Katz 1998). Interactions with the intracluster medium (ICM) have also remained a popular explanation of some of the properties of the Butcher-Oemler population (Gunn & Gott 1972).

The *HST* imaging of distant clusters also turned up evidence for evolution in the passive cluster galaxies. The population of luminous cluster ellipticals appears to have

[2] Institute of Astronomy, Madingley Road, Cambridge CB3 OHA, UK.

[3] Royal Greenwich Observatory, Madingley Road, Cambridge CB3 0EZ, UK.

[4] Osservatorio Astronomico di Padova, vicolo dell'Osservatorio 5, 35122 Padova, Italy.

[5] Department of Physics, University of Durham, South Road, Durham DH1 3LE, UK.

[6] The Observatories of the Carnegie Institution of Washington, 813 Santa Barbara Street, Pasadena, CA 91101-1292.

[7] School of Physics, University of New South Wales, Sydney 2052, Australia.

[8] Institute for Astronomy, University of Hawaii, 2680 Woodlawn Drive, Honolulu, HI 96822.

[9] NFRA, P.O. Box 2, 7990 AA Dwingeloo, The Netherlands.

been in place in the clusters since at least $z \sim 0.6$ (Smail et al. 1997b), and the homogeneity of their properties would argue that they underwent the bulk of their star formation prior to $z \sim 3$ (Bower, Lucey, & Ellis 1992; van Dokkum & Franx 1996; Ellis et al. 1997; Barger et al. 1998). In contrast, the S0 galaxies that dominate the cores of rich clusters today are noticeably absent from these environments at $z \sim 0.5$ (Dressler et al. 1997). The recent formation or transformation of the cluster S0 galaxies and the connections to the evolutionary history of the Butcher-Oemler population are of considerable interest for understanding the extent of environmental influences on galaxy morphology and stellar populations.

To elucidate the physical processes that are driving the star formation activity and morphological transformations in these distant clusters, we have been conducting a large space- and ground-based study of 10 rich clusters in the range $0.37 \leq z \leq 0.56$. One of the main aims of this study— known as the "MORPHS" collaboration—has been to obtain detailed morphologies of magnitude-limited samples of galaxies in these clusters from high-resolution images taken with the Wide Field and Planetary Camera 2 (WFPC2) on board the *HST*. These data have already been presented and discussed in a series of papers (Smail et al. 1997a, 1997b; Ellis et al. 1997; Dressler et al. 1997; Barger et al. 1998).

Another important component of our program has been to obtain extensive ground-based spectroscopy within the fields of these clusters in order to better quantify the star formation activity of the cluster galaxies, particularly those for which *HST* morphologies are available. In Dressler et al. (1999; hereafter D99) we presented spectra for 657 galaxies observed across the fields of our 10 clusters, 424 of which were confirmed to be cluster members. Detailed morphological and photometric information from the *HST* images (Smail et al. 1997b, hereafter S97) is available for 204 cluster members and 71 field galaxies and has been included in the D99 tables. This data set is suitable to study simultaneously the spectral and morphological properties of galaxies in distant clusters, and it allows a direct comparison between the high-redshift field and cluster populations. The main results of D99 can be summarized as follows:

1. The poststarburst (k + a/a + k) galaxies are a significant fraction, $\sim 20\%$, of the cluster population, while their incidence in the field at similar redshifts is considerably lower. Moreover, the frequency of k + a/a + k galaxies in clusters is much higher at $z = 0.4$–0.5 than at low redshift and apparently evolves more strongly with redshift than in the field population. While the galaxies in this class include examples of all Hubble types, the majority of them show disk-dominated morphologies.

2. At a given Hubble type, the cluster galaxies show a higher frequency of spectra with low or no detectable [O II] emission compared with the surrounding field (including examples of late-type spirals with no current star formation). This indicates a general reduction in the star formation activity of galaxies in the clusters, as measured by the EW([O II]), compared with the field.

3. Those galaxies that are currently forming stars (all the spectral classes with emission lines) have both a more extended spatial distribution and a higher velocity dispersion than the galaxies with passive (k-type) spectra. The recently star-forming k + a/a + k galaxies exhibit spatial and kinematic distributions intermediate between the

passive and active populations. Dressler et al. (1999) interpret the kinematic and evolutionary behavior of the poststarburst galaxies as clear evidence for the environment being responsible for the formation or visibility of the k + a/a + k classes.

D99 gave a qualitative discussion of the properties of the cluster galaxies and laid the groundwork for the quantitative analysis undertaken in this work. The purpose of this paper is to model and interpret the different spectroscopic classes in D99 in order to identify the star formation patterns that are present in cluster galaxies at these earlier epochs and thus predict their likely subsequent (and also previous) spectrophotometric evolution. This information is vital to detailing and therefore understanding the physical processes responsible for the changes in luminosity, color, and morphology that underlie the "Butcher-Oemler" effect. It is worth stressing that, although the existence of a strong evolution between $z \sim 0.4$–0.5 and $z = 0$ is well established, a data set equivalent to the one presented in D99 does not exist for low-redshift clusters, and this of course limits the comparison with the present epoch.

The plan of this paper is as follows: in § 2 we describe the different spectroscopic classes found in the distant clusters and examine the possible selection effects that influenced their inclusion in the spectroscopic sample. In § 3 we model and interpret each spectroscopic class separately; in this section we also examine whether analogous systems exist in the local universe and what these can tell us about the effects of dust extinction on the spectral properties of starburst galaxies. In § 4 we analyze the predicted range of spectrophotometric paths of each class and investigate the possible evolutionary connections among the classes. We then use our sample of spectra for similarly distant "field" galaxies to compare the star formation activity in and out of clusters at this epoch, and we combine what has been learned on the star formation activity of the different classes with their *HST* morphologies, looking for connections between the two. In § 5 we also examine whether star formation activity in distant clusters is correlated with global cluster properties, and we then summarize our main conclusions in § 6. Unless otherwise stated, we assume $q_0 = 0.5$ and take $h = H_0/100 \text{ km s}^{-1} \text{ Mpc}^{-1}$.

2. THE SPECTROSCOPIC CATALOG

In this section we briefly outline the spectral classification scheme adopted in D99 and analyze the possible selection effects in this sample. Our classification scheme is based primarily on two lines, [O II] $\lambda 3727$ and Hδ ($\lambda = 4101$ Å), which are good indicators of (respectively) current and recent star formation (SF) in distant galaxy spectra. All the equivalent widths in this paper are given in angstroms in the rest frame and with a negative value when in emission.

The spectral classification scheme is presented in Table 1, taken from D99. A full explanation of the notation denoting the various spectral classes can be found in D99. Only 62 out of the 657 spectra were too poor to be assigned a spectral class, and in 38 of these at least one emission line could be identified. Thus we have spectral classifications for around 95% of our sample.

For the purposes of this paper we have also divided the Balmer-strong galaxies with no emission (k + a/a + k type) into "blue" and "red" galaxies (as was done in CS87 for the poststarburst galaxy and red Hδ-strong classes, respectively); in this case the color threshold has been

TABLE 1
SPECTRAL CLASSIFICATION SCHEME FROM D99

Class	EW [O II] $\lambda 3727$ (Å)	EW Hδ (Å)	Color	Comments
k	absent	<3	...	passive
k + a......	absent	3–8	...	moderate Balmer absorption without emission
a + k......	absent	≥8	...	strong Balmer absorption without emission
e(c)	yes, <40	<4	...	moderate Balmer absorption plus emission, spiral-like
e(a)	yes	≥4	...	strong Balmer absorption plus emission
e(b)	≥40	...	...	starburst
e(n)	...	...	...	AGN from broad lines or [O III] 5007/Hβ ratio
e	yes	?	...	at least one emission line, but S/N too low to classify
?...........	?	?	...	unclassifiable
CSB	...	...	very blue	photometrically defined starburst

chosen to be $(g - r) = 1.15$ (in the observed frame at $z = 0.4$), equivalent to the one adopted in CS87 ($B_J - R_F = 2$ at $z = 0.31$), and it corresponds to the separation between the expected color of the early-type galaxies (Sa or earlier) from the later-type spirals and irregulars (Sb and later). The Galactic extinction in the direction of the clusters in our sample is negligible (S97), except in the case of Cl 0303 + 17 [$E(B-V) = 0.12$], and no reddening correction has been applied in this paper.

The Balmer-strong population is evident in Figure 1, which shows EW(Hδ) as a function of the observed $(g - r)$ color for cluster and field galaxies. Such a diagram was presented for the first time for a large spectroscopic data set in three clusters at $z = 0.31$ by CS87. The k + a/a + k galaxies stand out as a numerous population both at red and blue colors [*filled dots*, with EW(Hδ) > 3 Å], as seen in previous spectroscopic surveys. The e(a) galaxies [*crosses*, with EW(Hδ) > 4 Å] dominate the blue side of the diagram, together with the e(c) galaxies [most of the *crosses*, with EW(Hδ) < 4 Å]. The k class, represented by the filled dots with EW(Hδ) < 3 Å, have red colors consistent with their

passive spectrum. The difference in Figure 1 between the cluster and field diagrams is striking, and we will discuss it in § 5.1; the field is missing the large population of k + a/ a + k galaxies, while a large number of e(a) spectra are still present (D99).

2.1. Sample Selection

The selection of the spectroscopic targets was influenced by galaxy morphology within the core region covered by the WFPC2, while outside this area the catalog is essentially a magnitude-limited sample to $i \sim 21$ mag (D99). The comparison between D99 and the morphological catalog (S97) allows us to quantify this effect and apply the appropriate corrections. For each cluster we compared the fraction of a given morphological type in the spectroscopic catalog (including both cluster members and field galaxies in each cluster field) with the proportion observed in the *HST* catalog (S97) down to the limiting magnitude in D99. The ratio of these two fractions gives the total (cluster + field) morphological correction factors. These have been subsequently partitioned between cluster and
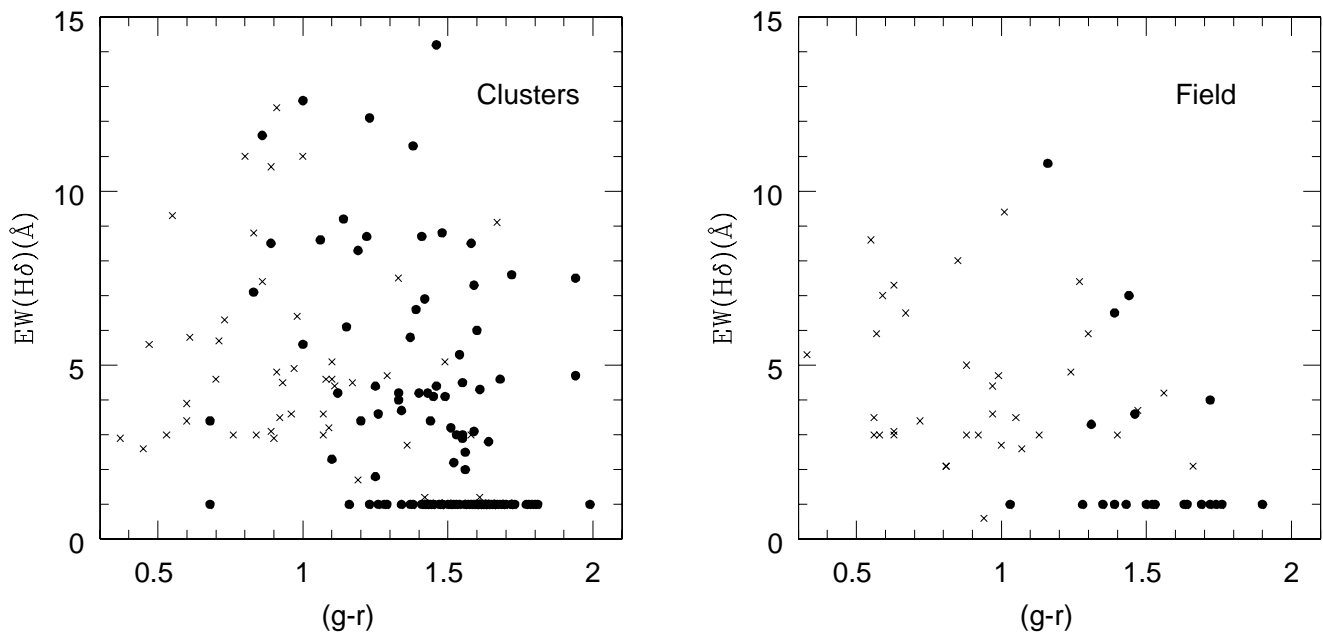

FIG. 1.—Color-Hδ diagrams for the cluster (*left*) and field (*right*) populations from D99. Crosses and circles indicate spectra with and without emission lines, respectively. Only members with $r < 22.5$ are presented in the plot. The "e(n)," "e," and uncertain (:) spectral classes are excluded. If not measured, the EW(Hδ) of k-type galaxies have been set equal to 1 Å. The $(g - r)$ color has been K-corrected to $z = 0.4$.

TABLE 2
MORPHOLOGICAL CORRECTION FACTORS

Cluster	E	S0	Sd/Irr
Cl 1447+23	1.43	...	...
Cl 0024+16	1.76	1.83	0.42
Cl 0939+47	1.26	1.62	0.93
Cl 0303+17	1.31	1.09	0.39
3C 295	2.79	1.74	0.51
Cl 1601+42	1.19	2.18	...
Cl 0016+16	1.88	2.55	0.46
Average clusters	1.61	1.75	0.60
Field	1.55	1.91	0.34

field galaxies to find the final morphological corrections we have applied to the distributions in D99. The number of galaxies of a given Hubble type in the spectroscopic catalog needs to be multiplied by these factors, given in Table 2, in order to find the "true" number that would have been observed in an unbiased sample. The table shows that, for the inner regions of the cluster, the Sd/Irr galaxies are slightly oversampled relative to the Sa–Sc types, while the E/S0 population is slightly undersampled. The values in Table 2 are normalized taking the correction factor for Sa, Sb, and Sc galaxies equal to 1; the morphological types have been classed according to the following T types: E (T types from -6 to -4 both included), S0 (-3, 0), Sa (1, 2), Sb (3, 4), Sc (5, 6), and Sd/Irr (7, 10). Three fields have not been included in this table: Cl 0054−27 and Cl 0412−65, for which the number of good quality spectra is too small, and the outer field in A370. To estimate the correction to the spectral classes we then weight these factors by the observed distribution of spectral classes within each morphological type (Table 3).

In the same way we have checked for any bias in the spectroscopic catalog related to the degree of distortion or disturbance of the galaxy's structure, as measured by the disturbance index D (S97). Such a bias is not present in our sample, and after having corrected for the morphological bias in the central fields, the whole spectral data set represents an essentially magnitude-limited sample. All the results presented in this work have been corrected for these selection effects.

We note that the spectroscopic sample analyzed here is roughly limited at an absolute magnitude of $M_V = -19 + 5 \log_{10} h$ or $M_V^* + 1.5$ (D99), while the morphological catalog on which our sample is based reaches down to $M_V^* + 3.5$; this itself is 3 mag brighter than the 5 σ detection limit of the WFPC2 imaging data at the median cluster redshift (S97). The continuity in the sample properties for the galaxies in the full (deeper) morphological catalog compared with the spectroscopic subsample suggests that the latter is not missing large classes of galaxies due to surface brightness selection limits, although we cannot rule out a subtle bias resulting from the original object selection.

3. THE INTERPRETATION OF THE SPECTRAL CLASSES

In this section we model and interpret each spectroscopic class in isolation before attempting to establish possible evolutionary relations between the various classes (§ 4). In some cases we will also examine the properties of low-redshift galaxies with similar spectra to provide further insights into the physical processes that are signposted by particular combinations of spectral features. In all of this our aim is to constrain, on the basis of the observed spectra, the past and present (and future) star formation history of these galaxies.

All the models employed in this paper have been generated with the spectrophotometric code of Barbaro & Poggianti (1997). This code has a number of advantages for the purpose of our study; in particular it includes both the contribution of the stellar component and the thermal emission of the ionized gas in H II regions.

The stellar component is computed by an evolutionary synthesis model that takes into account the main evolutionary phases up to the asymptotic giant branch (AGB) and post-AGB. The stellar model allows us to compute the integrated spectral energy distribution (SED) at low resolution over a wide wavelength range (20 Å, 1000–25,000 Å) and at higher resolution across a shorter interval (4 Å, 3500–7500 Å). The first version, based on Kurucz stellar atmosphere models (Kurucz 1993), is suitable for computing colors and studying low-resolution features (such as the 4000 Å break) with a wide wavelength coverage and including stellar populations of different metallicities. The second version, based on the stellar spectral library observed by Jacoby,

TABLE 3
FRACTION OF GALAXIES OF A GIVEN HUBBLE TYPE AS A FUNCTION OF SPECTRAL CLASS

Morphology	N_{tot}	k	k + a	a + k	e(a)	e(c)	e(b)	e(n)	e	?
					Cluster Sample					
E	54	0.81 ± 0.12	0.09 ± 0.04	0.02 ± 0.02	0.02 ± 0.02	0.04 ± 0.03	0	0.02 ± 0.02	0	0
S0	24	0.62 ± 0.16	0.21 ± 0.09	0.04 ± 0.04	0	0.08 ± 0.06	0	0	0	0.04 ± 0.04
Sa	39	0.69 ± 0.13	0.13 ± 0.06	0.03 ± 0.03	0.05 ± 0.04	0.05 ± 0.04	0	0	0	0.05 ± 0.04
Sb	38	0.29 ± 0.09	0.21 ± 0.07	0.08 ± 0.05	0.13 ± 0.06	0.13 ± 0.06	0	0.05 ± 0.04	0.08 ± 0.05	0.03 ± 0.03
Sc	29	0.17 ± 0.08	0.17 ± 0.08	0.10 ± 0.06	0.28 ± 0.10	0.10 ± 0.06	0.10 ± 0.06	0.03 ± 0.03	0.03 ± 0.03	0
Sd/Irr	20	0.10 ± 0.07	0.05 ± 0.05	0.05 ± 0.05	0.25 ± 0.11	0.15 ± 0.09	0.35 ± 0.13	0	0	0.05 ± 0.05
					Field Sample					
E	9	0.44 ± 0.22	0	0	0.22 ± 0.16	0.22 ± 0.16	0	0	0.11 ± 0.11	0
S0	6	0.33 ± 0.24	0.33 ± 0.24	0	0	0	0.33 ± 0.24	0	0	0
Sa	6	0.67 ± 0.33	0	0	0	0.33 ± 0.24	0	0	0	0
Sb	11	0.27 ± 0.16	0	0	0.09 ± 0.09	0.36 ± 0.18	0.09 ± 0.09	0	0.09 ± 0.09	0.09 ± 0.09
Sc	26	0.04 ± 0.04	0.04 ± 0.04	0	0.08 ± 0.05	0.54 ± 0.14	0.19 ± 0.09	0	0.08 ± 0.05	0.04 ± 0.04
Sd/Irr	13	0	0	0	0.15 ± 0.11	0.23 ± 0.13	0.15 ± 0.11	0	0.38 ± 0.17	0.08 ± 0.08

Hunter, & Christian (1984; mostly of solar metallicity), has enough resolution to study absorption features, such as the stellar lines of the Balmer series.

In studying star-forming galaxies it is particularly useful to reproduce the nebular emission lines, which are the most prominent features of the integrated spectrum and are directly related to the current star formation rate (SFR). The Kurucz-based version of the stellar model computes the ionizing flux (below 912 Å), which is used to derive the luminosities of the nebular Balmer lines assuming case B recombination (optically thick; Osterbrock 1989). The luminosities of a number of metallic lines, including [O II] $\lambda 3727$, are computed using the grid of H II region models given by Stasinska (1990). The emission-line spectrum is obtained assuming solar metallicity gas, and all the model equivalent widths have been measured using the same software that was used on the data.

Figure 2 shows the various types of star formation histories we have considered, which include spiral-like models (a), truncated models (b), truncated models with a burst (c), and spiral-like models with a burst (d). The SFRs and properties of the spiral-like models have been published in Barbaro & Poggianti (1997) and resemble the set of SF histories described by Sandage (1986), where the ratio of present-to-past average SF increases toward later types. They correspond to the Bruzual & Charlot μ models with a wide range of SF timescales (τ); in particular, we have investigated a set of models with τ between 0.5 Gyr and ∞ (constant SFR), including also a model whose SFR constantly increases with time.

3.1. The k + a/a + k Class—a Review

A large amount of theoretical work has been devoted to the interpretation of k + a/a + k spectra (Dressler & Gunn 1983; CS87; Henry & Lavery 1987; Newberry, Boroson, & Kirshner 1990; Belloni et al. 1995; Barger et al. 1996; Poggianti & Barbaro 1996; Morris et al. 1998). The main conclusions can be summarized as follows:

a) A spectrum with strong Balmer lines in absorption [EW(Hδ) > 3 Å] and negligible emission lines belongs to a galaxy that has no significant current SF but was forming stars in the recent past (<1.5 Gyr). Strong (Hδ) equivalent widths [EW(Hδ) > 4–5 Å] can only be reproduced by models seen in a quiescent phase soon after a starburst; for this reason k + a/a + k spectra are often identified with "poststarburst galaxies." Moderately strong Balmer lines [EW(Hδ) < 4–5 Å] can also be obtained by simply halting the star formation in a galaxy that was forming stars in a regular, continuous manner (truncated models), but the exact threshold between these two regimes is not well defined, since it is affected by the uncertainties in the measurement of the EW, both in the data and in the models. Newberry et al. (1990) showed that truncated, as well as burst, models could reproduce the properties of passive, Balmer-strong galaxies seen in the first spectroscopic surveys, which gave much looser constraints than subsequent data. More recently, truncated models without a starburst have been advocated by Morris et al. (1998), although their definition of a "truncated model" is different from the one generally adopted. In fact, they consider a 1 Gyr period of constant star formation, followed by a complete cessation of the SF; such a model reproduces high EW(Hδ) during a period of 1–2 Gyr after the halting of the SF. In this model the galaxy did not form any star before
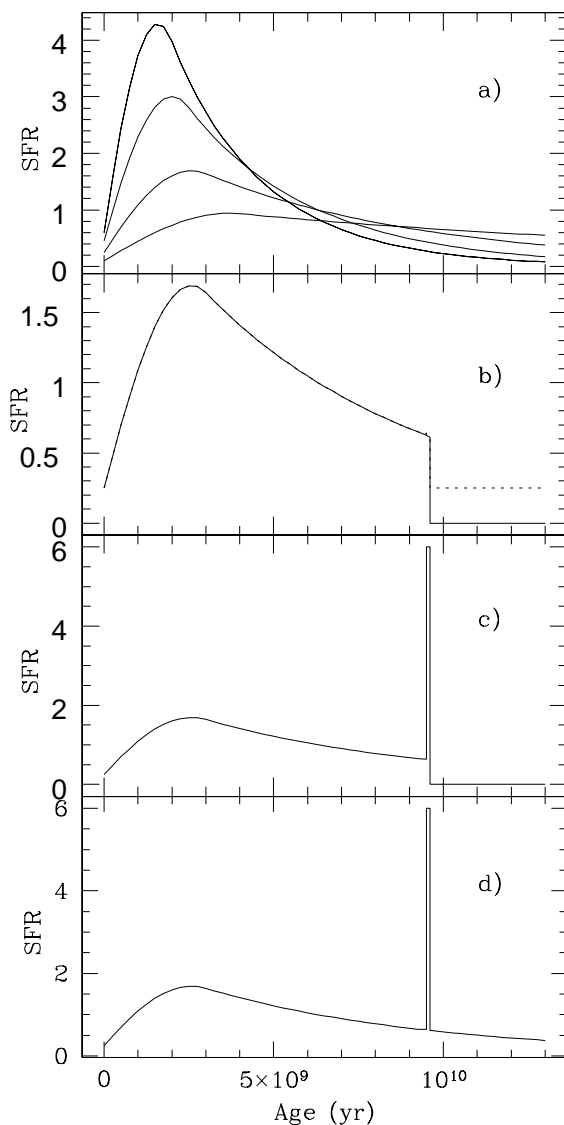

FIG. 2.— Star formation histories of the various classes of models. SF rates are in arbitrary units: (a) Spiral-like models (Barbaro & Poggianti 1997), simulating an "Sa" (upper curve, at zero age), "Sb," "Sc," and "Sd" galaxy (lower curve). The model parameters were determined by requiring the SED to reproduce at an age of 16 Gyr the average observed colors and gas fraction of present-day galaxies (Barbaro & Poggianti 1997); the chemical evolution was computed with a simple model with inflow that assumes the SFR to be proportional to the gas fraction. (b) Truncated models. The solid line shows the spiral-like "Sc" model where the star formation is suddenly halted. The dotted line represents the case in which some residual SF remains after the abrupt decrease. (c) Truncated models with burst. The spiral-like "Sc" model, after a strong burst lasting 0.1 Gyr, has no further SF. (d) A burst is superposed on a spiral-like ("Sc") SF history. At the end of the burst, a regular SF is resumed.

the 1 Gyr constant SF (1–3 Gyr before the Hδ-strong phase) and using the definitions commonly employed in the literature, this is a "poststarburst" model where the burst involves 100% of the galactic mass.

b) The last star formation event ended between a few Myr and 1.5 Gyr before the time of observation. This range of timescales is determined by the lifetime of the stars responsible for the strong Balmer lines (Poggianti & Barbaro 1997).

c) Spectral models using a standard Salpeter initial mass function (IMF) show that a significant fraction of the galac-

tic mass needs to be involved ($>10\%–20\%$) in the recent star formation episode in order to explain the highest EW(Hδ) typically observed. In fact, the most extreme cases [EW(Hδ) > 10 Å] can hardly be reproduced with a standard IMF at all (Poggianti & Barbaro 1996; A. I. Zabludoff 1997, private communication).

d) The duration of any previous starburst phase is usually considered unconstrained, with the exception of the work of Barger et al. (1996), which found possible support for short-lived bursts (~ 0.1 Gyr).

e) The SF history *prior* to any burst cannot be determined from a poststarburst spectrum (unless ultraviolet data sampling around 1500 Å in the rest frame is available). However, the high mass fractions implied for the burst have always suggested that later-type galaxies are more likely progenitors, owing to their higher gas fractions (Poggianti 1994). This suggestion has received support from the *HST*-based morphological studies (Couch et al. 1994, 1998; Dressler et al. 1994, 1999; Oemler et al. 1997; S97), which typically show that the morphologies of the poststarburst population are predominantly disk dominated.

f) The spectral properties *after* the k + a/a + k phase depend of course on the subsequent SF history: if no SF is resumed, the signature of the latest star formation episode (i.e., the strong Hδ) eventually disappears around 1–1.5 Gyr after the end of the star formation. After this the galaxy shows a k-type spectrum.

g) All the spectroscopic surveys, including D99, identify a group of galaxies with very strong Hδ *and* very red colors. These remain unexplained by the spectral models, which predict that the galaxies with strong Hδ should remain moderately blue, even as they decline to weaker Hδ strengths. For example, in Figure 1 they are the 13 cluster galaxies with ($g - r$) > 1.3 and EW(Hδ) > 5 Å, lying in a part of the Hδ-($g - r$) plane that cannot be reached by any simple poststarburst model (CS87; Poggianti & Barbaro 1996; Barger et al. 1996; Morris et al. 1998). This discrepancy could be due in part to uncertainties in the zero-point matching of the observational and theoretical photometric systems (presumably 0.1–0.2 mag at most), as well as the result of observational errors. Nevertheless, it is unlikely that these effects are responsible for all the galaxies observed in this region of the diagram. Couch & Sharples (1987) and Morris et al. (1998) discuss possible solutions to the problem, which include internal reddening, supersolar metallicities, or a top-heavy IMF for the stars produced during the recent star formation. However, a definitive conclusion has not been reached so far, and we will address this issue later, in § 4.

3.2. *The* e(b) *Class*

Our models show that EW([O II]) $= 40$ Å cannot be reached with a spiral-like star formation history. We have explored the set of star formation histories shown in Figure 2*a*, and even models with constant or constantly rising SFR do not reach EWs greater than 40 Å, which seem to require a burst of star formation. However, it should be kept in mind that the emission models are for solar metallicity H II regions and that the relation between SFR and [O II] flux changes substantially with metallicity. Although their strong emission lines testify to a high current SFR, the interpretation of these galaxies as "starbursts" is not straightforward: the [O II] equivalent widths of the e(b) galaxies

have values comparable to the very late type spirals/ irregulars at low redshift (Kennicutt 1992a, 1992b), and even for the nearby galaxies it is still a matter of debate whether they are able to sustain the current SFR for an extended period of time and whether the are experiencing a continuous or an episodic SF history.

In order to better understand the nature of the e(b) galaxies in our sample, we have estimated their metallicities using the R_{23} index, which is a ratio of line fluxes (Pagel et al. 1979; Edmunds & Pagel 1984): $R_{23} = ([O\ II]$ $\lambda 3727 + [O\ III]$ $\lambda\lambda 4959, 5007)/H\beta$. The measured abundances of the e(b) galaxies (Appendix) are significantly lower than those of any other spectral class and are comparable to those in low-luminosity, very late type spirals and the most luminous irregulars at low redshift.

3.3. *The* e(c) *Class*

By definition, the e(c) spectra are similar to those of typical present-day spirals: they are defined to have weak-to-moderate [O II] $\lambda 3727$ emission ([O II] detected, but with EW([O II]) < 40 Å) and weak-to-moderate Hδ absorption [EW(Hδ) < 4 Å]. This broad range in emission- and absorption-line strength has been chosen to encompass the observed characteristics of all the normal spirals of Sa type or later in the sample of nearby galaxies of Kennicutt (1992a, 1992b). The spiral-like model spectra used in this paper (some of which are shown in Fig. 2*a*) fall in this spectral class.

The modeling also shows that there is an alternative way of reproducing an e(c) spectrum: starbursts of sufficiently long duration ($\gg 0.1$ Gyr) can in their later phases mimic the e(c) classes. After an initial e(b) phase with very strong emission lines lasting ~ 0.1 Gyr, the starbursting galaxy displays an e(c) spectrum as long as the star formation continues. This is shown in Figure 3 for a burst model as in Figure 2*c*, in which the burst lasts 1 Gyr and ends at $\tau = 0$ with no further SF.

In this model ~ 20 % of the galactic mass is turned into stars during the burst, but the SFR in the starburst phase (assumed to be constant) is just 3 times the rate before the burst begins. Of course at this level the use of the term "starburst" is arbitrary: for this model the timescale for gas exhaustion is not a small fraction of the Hubble time.

3.4. *The* e(a) *Class*

The e(a) class includes all the galaxies with EW(Hδ) > 4 Å and measurable [O II] emission. We have chosen to treat these as a separate class from the e(c) spectra because their Hδ line is too strong compared with those of normal low-redshift galaxies of any Hubble type (Kennicutt 1992a). Further suggestions of the unusual nature of this class come from our modeling of exponentially decaying SFR, with a range of timescales, which confirms that a continuous SF history does not produce spectra with a net EW(Hδ) > 4 Å in absorption when the emission filling is taken into account.

In the D99 spectroscopic catalog there are 44 e(a) spectra out of a total of 399 cluster members with an assigned spectral class. The fraction of e(a) spectra in the magnitude-limited sample is around $\sim 10\%$. Although spectra with these characteristics are present in other spectroscopic surveys of distant clusters (e.g., CS87; Couch et al. 1994, 1998; Fisher et al. 1998), their relevance and interpretation have not been extensively discussed in previous works. We
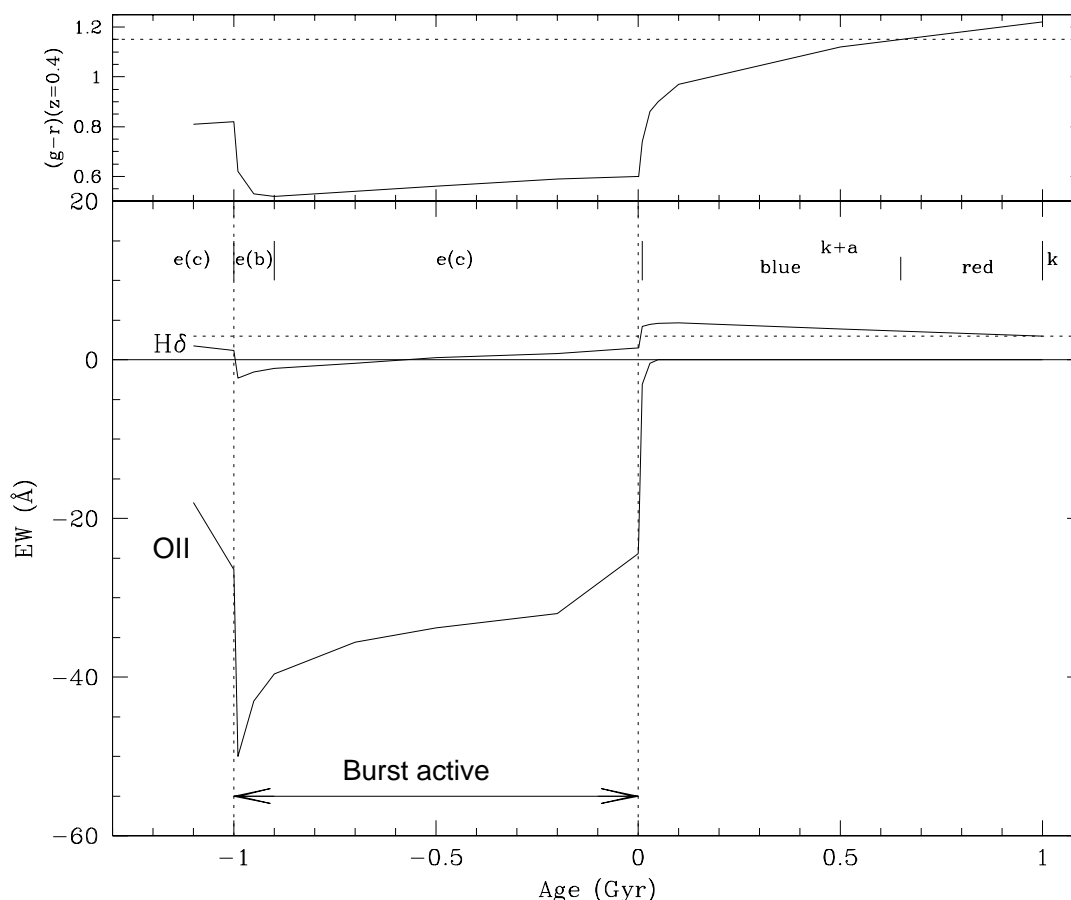
FIG. 3.—Modeling of a "long burst." The plot shows the evolution of the [O II] and Hδ equivalent widths during and after a burst lasting 1 Gyr and ending at $\tau = 0$. The two dotted vertical lines delimit the period of the burst. The k + a model spectra lie above the dotted horizontal line at EW(Hδ) = 3 Å. The spectral classification at each stage is shown in the top part of the lower panel, including the distinction between blue and red k + a phase. For ages less than -1 Gyr a "spiral-like" model is assumed (Fig. 2a). The top panel shows the $(g - r)$ color if the galaxy was observed at $z = 0.4$ at any time. The dotted line in the top panel represents the limit between red and blue galaxies.

now present dust-free modeling of this spectral class, followed by a discussion of the role of dust in defining the characteristics of low-redshift galaxies with e(a) spectra.

Since the e(a) spectra display emission lines, only models with active star formation at the time of observation have been considered; an extensive region of parameter space and various star formation histories have been investigated (Fig. 2). The spectral characteristics of e(a) galaxies can be reproduced assuming that, after a recent strong starburst, the galaxy resumes a much lower SFR. Both of these properties (recent burst and a low current SFR) are necessary to explain the observed spectra.

Models with a regular, smooth SF history, with no burst and no truncation (Fig. 2a), never reach EW(Hδ) > 2–3 Å, even for the SEDs typical of later morphological types. Truncated models (Fig. 2b, solid line) cannot reproduce the [O II] line, since they lack any present star formation.

We also investigated a class of models in which a spiral-like SFR drops to a much lower, but nonzero, level without experiencing a starburst (Fig. 2b, dotted line). All the models of this class have EW(Hδ) < 4 Å, and therefore they are unable to reproduce e(a) spectra.

Models with truncated SF at the end of the burst (Fig. 2c) also experience a very short e(a) phase; however, this phase is far too short to account for the large number of e(a)'s observed, and furthermore the EW([O II]) of these models is generally weaker than the observed values.

The only class of dust-free models that reproduce the strong Hδ in absorption and the [O II] in emission are poststarburst galaxies with some residual SF (Fig. 2d). As in the case of the k + a/a + k galaxies, the high EW(Hδ) requires a high fraction of the galactic mass to be involved in the burst (typically 20% or more for a standard IMF), and this result is independent of the burst duration, as long as it is less than 1 Gyr. We will see that this interpretation of the e(a) spectra predicts a bright phase with strong emission lines [e(b) spectrum] that is not observed.

Figure 4 shows a sequence of models at 0, 0.01, 0.1, 0.5, 1, and 2 Gyr after the end of a strong burst of SF (about 35% in mass), lasting 0.1 Gyr and superposed on a spiral-like "Sc" SF history. This is a model of the type shown in Figure 2d, in which at the end of the burst the galaxy resumes the regular spiral-like SFR and during the burst the SFR is 100 times the rate of the undisturbed galaxy. The model starts with an e(b) spectrum ($\tau = 0$, where τ is the time elapsed since the end of the burst) with strong emission lines, including Hδ in emission; at $\tau = 0.01$ Gyr the emission has already decreased significantly, and the Hδ line is quickly moving toward high EW in absorption [e(c)/e(a) spectrum]. The galaxy is an e(a) at $\tau = 0.1$ Gyr, and it remains in this spectral class until $\tau = 1$ Gyr, when the EW(Hδ) in absorption begins to decrease: from this moment on the galaxy has an e(c) spectrum as long as there is ongoing star formation. This model remains blue
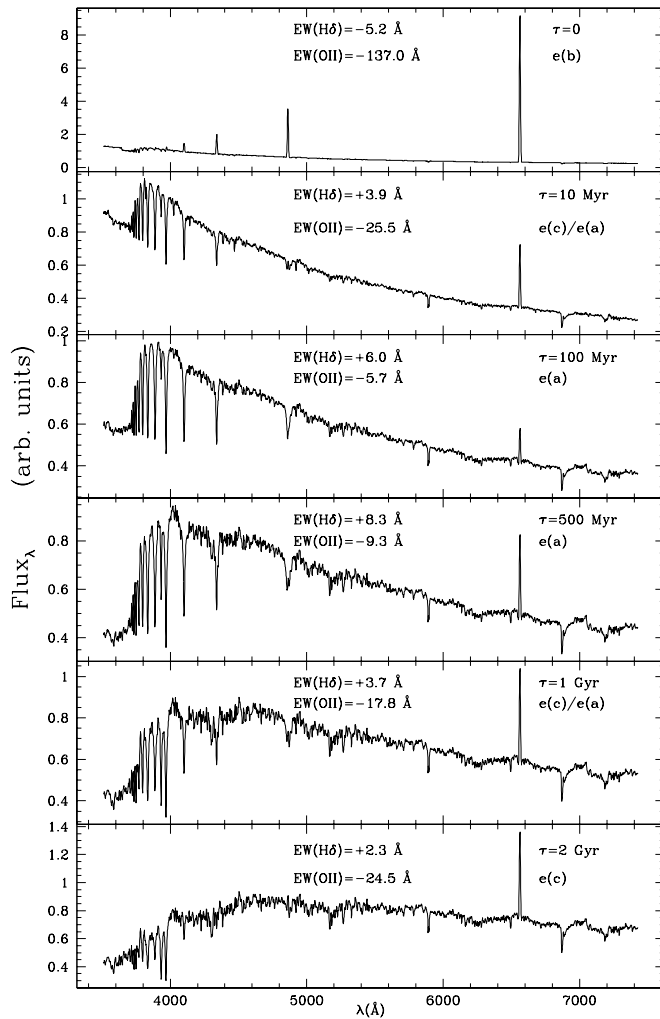
FIG. 4.—Spectra of a burst model with residual SF (Fig. 2d). The value τ is the time elapsed since the end of the burst.
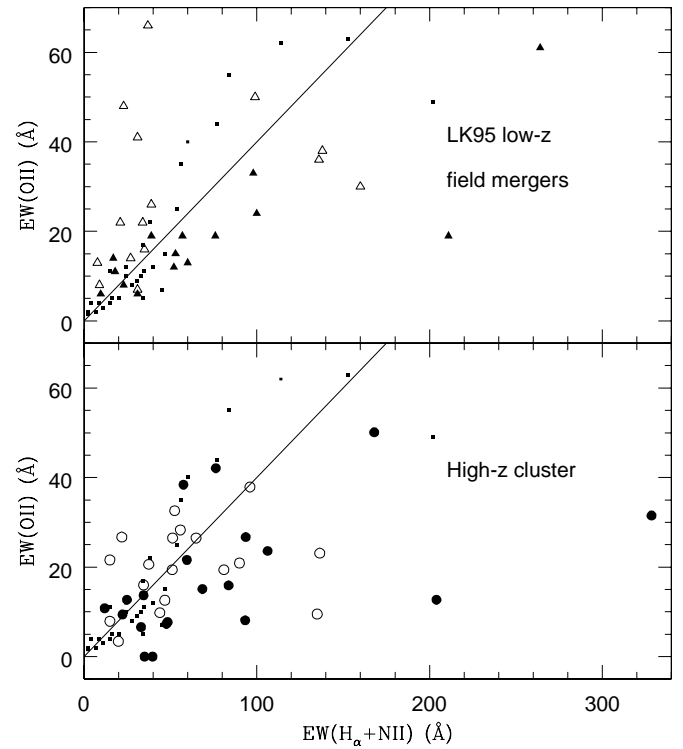

FIG. 5.—Comparison of the LK95 sample of merging galaxies with our distant cluster sample. Filled symbols represent e(a) spectra. In the top panel open triangles represent merging galaxies of non-e(a) spectral class, while in the lower panel the open circles are cluster members with e(c) spectra. In the distant cluster members the measured EW(Hα) has been multiplied by a factor 1.5 if the [N II] line was not already included in the measurement, assuming [N II]/Hα ≃ 0.5 on average (Kennicutt 1992b). The distant cluster e(c) galaxies are distributed equally about the fit for normal galaxies in the local universe (Kennicutt 1992a, 1992b; *small filled rectangles*), as expected if they are the counterparts of normal local spirals. Both plots are uncorrected for extinction.

(according to the definition given in § 2) during the whole evolution.

Our dust-free models therefore suggest that e(a) spectra can be obtained whenever a strong burst of star formation is followed by continuing star formation at a low level. In this scenario e(a) galaxies are poststarburst galaxies, and they differ from the k + a/a + k population only by having some residual star formation. We now discuss the possibility that the e(a) galaxies themselves are in the strong burst phase, heavily obscured by dust.

3.5. *The Role of Dust*

The e(a) class is, among our spectral classes, the one that has been the least discussed and is probably also the least understood. To gain more physical insight into the nature of galaxies in the e(a) class we have searched for examples of this class of galaxy in the local universe. We find good examples of e(a) spectra in the spectral atlas of merging galaxies by Liu & Kennicutt (1995a, hereafter LK95; 1995b), which is composed of merging or strongly interacting systems, as judged by either optical or near-infrared imaging. We reanalyzed their spectra in the same manner as D99 and found that around 40% of their galaxies have an e(a) spectrum (16/39), while at most 7% (1/14) of the normal

(nonmerging, non-Seyfert) galaxies in Kennicutt (1992a, 1992b) show an e(a) spectrum.

The e(a) galaxies in the LK95 sample are known to be dusty, merging, starburst galaxies: they are all strong far-infrared (FIR) emitters, and many of them are classified as ultraluminous IR galaxies (ULIRGs, $\log_{10} L_{FIR} > 11.5$ $\log_{10} L_\odot$ according to the LK95 definition).[10] A more detailed comparison of the similarities of the distant e(a) class and the galaxies in the LK95 sample is possible using the ratio of [O II] and Hα emission-line strengths. The e(a) spectra, both in the local merging sample and in the distant clusters, tend to have lower EW([O II])/ EW(Hα + [N II]) ratios than normal galaxies: in Figure 5 they are represented by the filled symbols, and they are found preferentially below the relation EW([O II]) = 0.4EW(Hα + [N II]), valid for the normal galaxy sample of Kennicutt (1992a, 1992b). These low EW([O II])/ EW(Hα + [N II]) ratios can be explained as an effect of dust: the line emission comes from the H II regions, where the young stars are still embedded in large amounts of inter-

---

[10] The strongest ULIRGs are believed to be often the site of both powerful nuclear starbursts and active galactic nuclei (AGNs), with the fraction of AGNs increasing with the FIR luminosity, particularly at $L_{ir} > 10^{12.3} L_\odot$ (Sanders & Mirabel 1996; Duc, Mirabel, & Maza 1997; Kim, Veilleux, & Sanders 1998). While the connection between nuclear starbursts and AGNs in ULIRGs is still under debate, it is well established that strong starbursts occur in the nuclei of all the very luminous IR galaxies (Wu et al. 1998 and references therein).

stellar matter. In a very dusty environment, both lines suffer strong extinction, [O II] being more affected than Hα.[11] However, the continuum underlying the lines probably comes from stellar populations that are more widely distributed throughout the galaxy, and hence suffers a lower extinction than the lines. The net result is a lower ratio of the equivalent widths of the two lines. Another possible explanation for the low [O II]/Hα ratios is high excitation, but this is ruled out for our cluster sample of e(a)'s, which do not generally show strong [O III] λ5007 lines.

We can see from Figure 5 that using the EW(Hα) to estimate the current SFR for e(a) galaxies instead of EW([O II]) would tend to increase the apparent SFR by factors up to ≳2–3. This revision means that we should interpret the e(a) population as dusty starbursts[12,13] and that the SFR and histories derived for e(a) spectra from dust-free models (§ 3.4) are misleading. In contrast, the spec-

tral properties and [O II]/Hα ratios of the e(c) and the e(b) spectra do not show evidence for a high dust extinction, and the dust-free models discussed in §§ 3.2 and 3.3 can be considered appropriate.

In a dusty starburst a high fraction of the bolometric luminosity is emitted at FIR wavelengths, and since this is an optically selected sample, one might worry about biases in the selection of the e(a) sample relative to the other (less reddened) spectral classes.

The competing effects of dust and starbursts on the luminosities of the e(a) galaxies are complicated to investigate. The net effect depends on the details of the mixing of the dust with the young and old stars within the galaxy. For likely burst strengths we would expect a brightening during the peak of the burst phase of 1–2 mag in the rest frame V band (Fig. 6). However, the observed ratio of Hα to [O II] equivalent widths suggests that the visual extinction to the emission-line regions is in the range 1.2–2.5 mag.[14] As the majority of the blue and visual luminosity resulting from the starburst is also likely to reside in these regions, we expect that the two effects will roughly cancel. Only after the stars have diffused out of these high-extinction regions will the dust become less effective, but the burst population will also have evolved and faded by this time.

---

[11] We note that there is the possibility that some of the non–emission-line spectra are actually e(a) galaxies with an extremely low [O II] line, where the Hα line is out of our spectrum, as it is observed in some cases in the Universidad Complutense de Madrid Survey (J. Gallego 1998, private communication).

[12] We note in passing that at least one e(a) cluster galaxy, 834 in Cl 0024+16, has been detected at submillimeter wavelengths, indicating a substantial dust content (Smail et al. 1998).

[13] Analysis of 123 spectra of Very Luminous IR galaxies (Poggianti & Wu 1999) from the sample of Wu et al. (1998) confirms the exceptionally high fraction (about 50%) of e(a) spectra among FIR-luminous galaxies.

[14] This is found adopting as *attenuation curve* the standard *extinction curve* of the diffuse medium in the Galaxy. We are forced to this arbitrary assumption by the lack of alternatives.
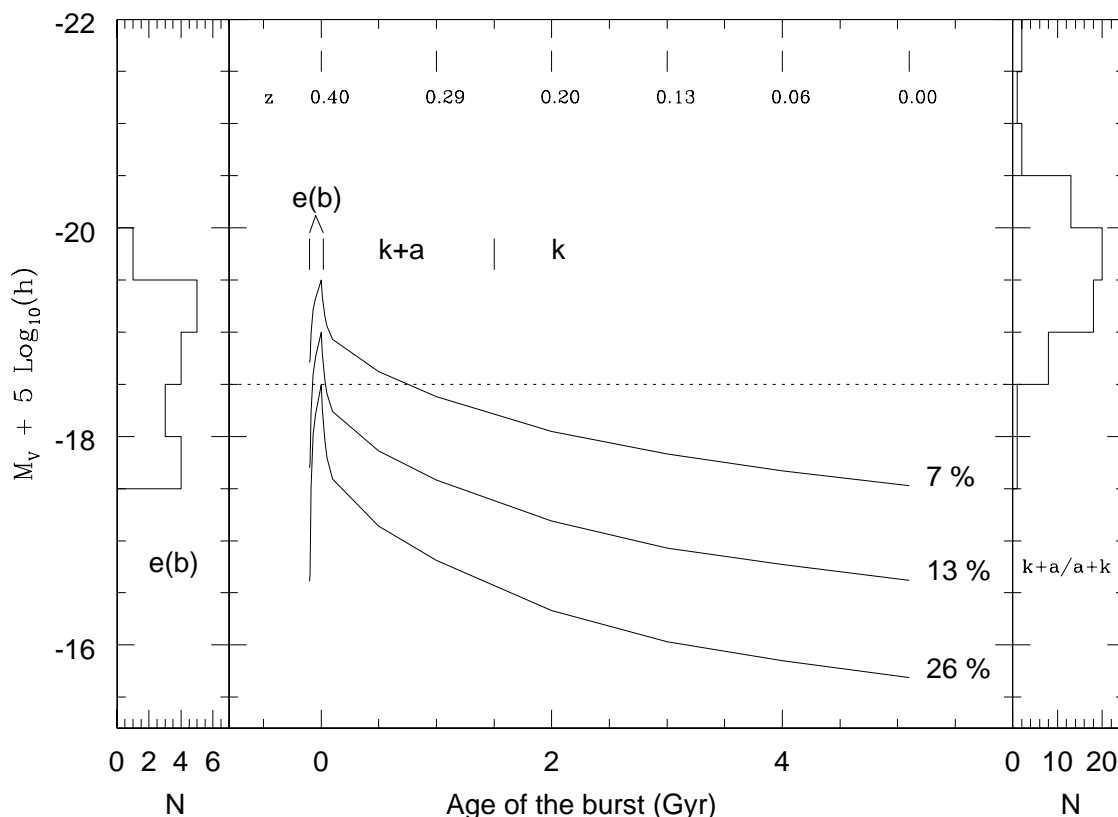

FIG. 6.—Evolution of the absolute V magnitude of three model galaxies that suffer a starburst and no subsequent star formation. The galactic mass fractions involved in the burst are shown on the right side of the plot; the flux from any emission line lying within the V band is not included. Lines start at the beginning of the burst, which lasts 0.1 Gyr and ends at τ = 0 taken to be z = 0.4. Prior to the burst a "late spiral-like" star formation history is assumed (Fig. 2c); this is a conservative choice that minimizes the luminosity evolution. The three models have been displaced arbitrarily at intervals of 0.5 mag at τ = 0 for display purposes. All of these models exhibit an e(b) spectrum during the burst, followed by a k + a phase lasting about 1.5 Gyr, and finally evolve into k galaxies. The dotted line shows the magnitude limit for k + a/a + k detection. The z-age relation is given for h = 0.5.

This cancellation suggests that there will be a relatively modest variation in optical luminosity for different burst strengths. Using the FIR luminosity as a tracer of the strength of the starburst, we see exactly this behavior at low z. In fact, a range of over 3 orders of magnitude in L_{FIR} for infrared-selected galaxies at low redshift is accompanied by less than a factor of 3–4 change in the optical luminosity (Sanders & Mirabel 1996). As an extreme case, the ULIRGs ($L_{FIR} > 10^{12} L_\odot$) have optical luminosities comparable to present-day L^* (Sanders & Mirabel 1996 and references therein). The FIR properties of our e(a) galaxies are probably less extreme, but even so their optical luminosities are not expected to be less than one-half to one-third of L^*. The D99 spectral catalog provides a representative luminosity distribution of cluster members at $M_V < -19 + 5 \log_{10} h$, 1.2 mag below the M_V^* of spiral galaxies at the cluster redshift (S97). We conclude that in general we expect the optical luminosities of the e(a) population to be crudely comparable to that expected for a nonbursting system. This suggests that there is no strong bias in our characterization of this population because of its dusty nature.

It is clear that galaxies with e(a) spectra appear in the low-redshift universe as well (see also Carter et al. 1988; Fig. 1 from Zabludoff et al. 1996; Gallego et al. 1997). Their frequency in the field at low z as estimated from the Las Campanas Redshift Survey (8%; Y. Hashimoto 1998, private communication) appears lower than in the distant field and clusters, although this comparison is an uncertain one because of the difference in the samples and the classification criteria.

At redshifts comparable to the D99 catalog, a population of Balmer-strong galaxies with emission is present in the field sample of the Canada-France Redshift Survey (see Fig. 15 in Hammer et al. 1997; Hammer & Flores 1998). Although a direct comparison cannot be made, their Balmer index versus D4000 plot is equivalent to our Figure 1, and the e(a) population is evident both at $0.5 < z < 0.7$ and $0.7 < z < 1$. This is in agreement with the results of the field sample in D99 (see § 5.2 and Fig. 1).

We will now try to identify the possible evolutionary paths among the spectral classes and hence discuss how the interpretation of e(a) spectra as dusty starbursts suggests they are good candidates for precursors of the k + a/a + k population.

4. PREDICTED EVOLUTION OF THE SPECTRAL CLASSES

We have seen in the previous section that the high proportion of k + a/a + k spectra observed in distant clusters indicates that a moderate fraction of cluster members were forming stars in the recent past but that this activity terminated at an epoch close to the time at which they are observed. In this sense their spectral properties indicate a sharp decrease in star formation activity. At the same time, in many cases the strong Hδ observed requires a burst of star formation prior to the sharp decline.

Given that the poststarburst models spend the second half of their k + a/a + k lifetime having more moderate Hδ strengths that progressively decline toward the 3 Å threshold (Poggianti & Barbaro 1996), at least some of the k + a/a + k spectra in the range $3 < \text{EW}(\text{H}\delta) < 5$ Å are expected to be the remnants of much stronger cases. Therefore, on the basis of standard IMF models, we find that a large fraction, possibly all, of the k + a/a + k galaxies in our sample are likely to have experienced a recent starburst. Although this fraction is surely significant, a quantitative estimate is problematic, given the uncertainty in the exact threshold between poststarburst and truncated models and the modest incompleteness of the sample for EW(Hδ) between 3 and 5 Å (D99).

The poststarburst interpretation of the k + a/a + k spectra necessarily poses the question of where are the starbursts, i.e., what is the progenitor population of the poststarburst galaxies? Our modeling shows that if no dust extinction is involved and a standard IMF is assumed, then the combination of a high SFR (required from the Balmer lines of the poststarburst galaxies) and short timescales (typical of starbursts) inevitably leads to emission lines with high equivalent widths. About 5% of our spectra show such strong emission lines [e(b) class], and therefore at face value these would be the most obvious candidate progenitors of the strong poststarburst k + a/a + k population.

We now show that the evolutionary scenario from e(b) to k + a/a + k spectra fails to account for the relative luminosity distributions observed for these two classes in the distant clusters. As discussed in D99, galaxies with e(b) spectra are conspicuously fainter than all the other spectral classes. Their typical luminosity range is also shown on the left side of Figure 6, which presents the expected luminosity evolution of a galaxy experiencing a burst and then no subsequent star formation. Assuming that the burst lasts 0.1 Gyr and ends at $\tau = 0$ in the plot—corresponding to $z = 0.4$—the absolute V magnitude evolves as shown for each of three different values of the galactic mass fraction of the burst (Δg).

Even for a modest Δg value, when the SF ceases, the model has already faded by 0.4–0.6 mag (depending on the intensity of the burst) at $\tau = 0.1$ Gyr, in comparison with the average magnitude during the e(b) phase. By the time the galaxy ends its k + a phase, it has faded by 1–1.5 mag.

We conclude that the bulk of the e(b) galaxies are not the progenitors of the k + a/a + k class we observed and that they do not evolve into any other spectral class visible in our sample: our analysis of their metallicities confirms that the properties of the e(b) galaxies resemble those of late-type, low-luminosity galaxies at low redshifts. If their destiny is to remain totally passive in their subsequent evolution, their spectral properties and magnitudes by $z = 0$ will be similar to those of passive dwarfs, as suggested by Koo et al. (1997; see also Wilson et al. 1997; Couch et al. 1998).

In § 3.3 we have seen that, in principle at least, some of our observed e(c) galaxies could be "long starbursts" and evolve into k + a/a + k galaxies later on, but it is more likely that these are simply galaxies that are forming stars in a regular, continuous manner with a spiral-like star formation history.

The question of whether an e(c) galaxy could evolve into a k + a *without* experiencing a starburst phase has been addressed in previous works (CS87; Newberry et al. 1990; Poggianti & Barbaro 1996). As discussed in § 3.1, models with a truncated star formation do evolve from e(c) to k + a but can only account for the weakest k + a types [EW(Hδ) < 5 Å] or at most half of our sample of k + a/a + k galaxies.

Another class of emission-line galaxies, e(a), is a better candidate for the progenitors of the k + a/a + k class. On the basis of dust-free models, the e(a) spectra appear associ-

ated with *poststarburst* galaxies with some residual star formation. If the SF eventually ceases, the spectrum evolves from the e(a) into the k + a/a + k class. The evolutionary sequence of this class of models starts presumably from an e(c) spectrum and ends up in a k + a/a + k or e(c) galaxy depending on whether the SF comes to an end:

$$e(c)(?) \Rightarrow e(b) \Rightarrow e(a) \begin{matrix} \nearrow e(c) \\ \\ \searrow k + a/a + k \Rightarrow k \end{matrix}$$
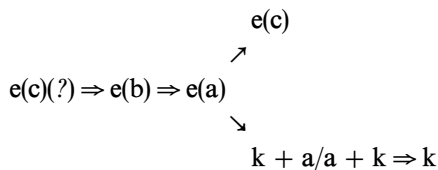
Although this evolutionary scenario is capable of interpreting an e(a) spectrum, this model implies a bright phase with strong emission lines [e(b) spectrum] that is not observed. In this model e(a) and k + a/a + k galaxies are poststarburst galaxies, and the only difference between these two classes is a low level of SF in the e(a) class.

However, the striking resemblance of our distant e(a) class with the spectra of low-z dusty starbursts and the analysis of their spectral properties, in particular, their low EW([O II])/EW(Hα) ratios, indicates that the e(a) galaxies are in fact starbursts which contain substantial amounts of dust and that dust-free models are unsuitable to estimate their star formation rates and histories.

We suggest that the e(a) galaxies, rather than the very rare bright e(b) galaxies, may be the missing link between the continuous star-forming galaxies and the poststarburst k + a/a + k class so abundant in the distant clusters. The e(a)'s and k + a/a + k's would then be galaxies in two distinct evolutionary phases, starburst and poststarburst, respectively. Identifying a strong Hδ line in emission-line spectra then represents a very powerful method to determine the incidence of a population of dusty star-forming galaxies up to high redshift and recognize the cases where the optically based SFR estimates are unreliable.

Furthermore, if the e(a) galaxies are dusty progenitors of the k + a/a + k galaxies, then it suggests that dust reddening might also affect the observed properties of some of the k + a/a + k galaxies. In particular, dust reddening may also be responsible for the class of very red k + a galaxies mentioned in § 3.1. As discussed there, these galaxies have broadband colors that are too red given the strength of the poststarburst features seen in the spectra. An internal reddening of $A_V = 0.5$ mag was found sufficient by CS87 to reproduce the reddest colors of the Hδ-strong population.

The absolute magnitude and color distributions (Fig. 7) as a function of the spectral class are consistent with the scenario outlined above. In fact the great majority of e(b)'s are very blue, most of the e(a) and e(c) types and a significant fraction of a + k are blue, while the great majority of k + a and k types are red. Figure 7 also shows that most of the blue galaxies responsible for the Butcher-Oemler effect are star-forming galaxies, since ~85% of them have emission lines: 13% e(b), 41% e(a), 31% e(c), 6% a + k, 6% k + a, 4% k. The original Butcher-Oemler magnitude and radius cutoffs have not been applied to derive these fractions. If the absolute magnitude cutoff is applied, the contribution of e(b) galaxies is drastically reduced.

To understand the environmental processes responsible for the poststarburst population and the connection between the spectrophotometric and the morphological
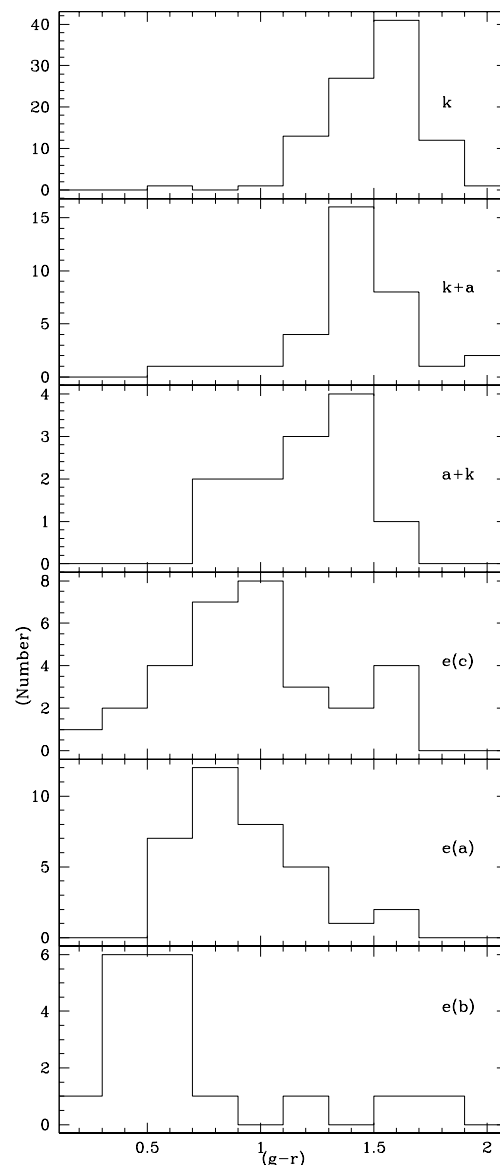

FIG. 7.—Color distribution as a function of the spectral class. All colors are K-corrected to $z = 0.4$.

evolution, we next discuss the properties of the different cluster populations in relation to their environments and morphologies from our *HST* imaging. Our aim is to search for ways to distinguish the underlying physical mechanisms at work in the formation of the k + a/a + k class, the k-type spiral galaxies, and more generally the S0 population (Dressler et al. 1997; van Dokkum et al. 1998).

5. ENVIRONMENTAL AND MORPHOLOGICAL TRENDS IN SF ACTIVITY

The basic relation between star formation and morphology for cluster galaxies in our sample has been presented in Dressler et al. (1999, their Fig. 7). They find that the passive k-type population is dominated by early-type galaxies, E and S0, but that it also contains a large number of later-type spirals, stretching out to Sd/Irr. The active cluster populations are typically populated by intermediate and late-type spirals: e(a) and e(c) are predominantly Sa–Sd/Irr galaxies, while e(b)'s are mostly Sc–Sd/Irr. The morphologi-

cal distributions of the poststarburst galaxies lie intermediately between the passive and active cluster populations: the a + k distribution is similar to that of the e(a)/e(c) galaxies, while the k + a distribution is relatively flat in types from E to Sc and therefore the k + a/a + k spectra mostly belong to spirals (as was found by Dressler et al. 1994; Wirth, Koo, & Kron 1994; Couch et al. 1998).

Looking at the distribution of spectral classes within each Hubble type, ellipticals, S0, and Sa galaxies have predominantly passive k-type spectra, with a tail of k + a/a + k and emission-line classes. Sb, Sc, and Sd/Irr galaxies show in most cases emission lines but still have an important fraction of k + a/a + k and k spectra that, although it decreases for later Hubble types, is still seen even in Sd/Irr galaxies. It is remarkable that only a small fraction (about 10%) of the spirals of types Sa–Sc in the core regions of the clusters have the spectral characteristics that are common in low-redshift normal spirals [e(c) spectrum]. The great majority are either "too active" [e(a) and e(b) classes, 22%] or "too inactive" (k + a/a + k and k classes, 25% and 43%, respectively).

5.1. Field versus Cluster Galaxy Properties

The great advantage of the spectral catalog in D99 is that it provides a direct comparison of the field and cluster populations at intermediate redshifts, which enables us to search for environmental variations in the properties of galaxies. The fraction of galaxies as a function of the spectral class are given for each cluster and for the total cluster and field samples in Table 4. They have been corrected for the morphological selection, and they are given as fractions of the total number of galaxies with assigned spectral class, excluding the e(n) class.

In contrast to the cluster environment, only a small proportion of the field spiral population falls into the k-type class, and these are typically early-type spirals. In the whole field sample more than half of the Sa–Sc spirals have an e(c) spectrum (54%), while the proportion of "too inactive" spirals is much smaller (5% k + a/a + k, 16% k), and the remaining 24% are e(a)'s or e(b)'s.

Although the distant clusters included in our sample do contain substantial populations of star-forming galaxies, it is also true that these emission-line galaxies are less common in the clusters than in the surrounding field (see Table 4). Moreover, at a fixed Hubble type, the frequency of galaxies with low or no measurable [O II] emission is significantly higher in the clusters (D99). If the cluster triggers the starbursts responsible for the strong k + a/a + k cases,

it must do this without significantly enhancing the [O II] emission (D99; see Balogh et al. 1997, 1998). This is conceivable, since the [O II] line is not a reliable indicator of current star formation in dusty galaxies [such as the e(a) galaxies in our interpretation], and the fact that the e(a) fraction in the cluster, although diluted by the passive preexisting population, is similar to the one in the field seems to suggest that the cluster environment is responsible for triggering some of the dusty starbursts. A definitive conclusion cannot be reached on the basis of the present sample because of the large statistical error bars on the observed fractions: comparing the field and cluster proportion of e(a) spectra in the supposedly recently infallen population (Sa to Sd/Irr), there is only weak (1 σ) evidence for a higher incidence of dusty starbursts in the clusters. Larger samples will be needed to assess the issue.

It is clear from the discussion above (see also Fig. 1) and in D99 that the most striking feature of the galaxy populations in the cores of distant clusters, especially when compared with the field at the same epoch, is not so much the presence of star-forming galaxies in this environment but rather the large population of galaxies that exhibit poststarburst features in their spectra: the k + a/a + k class. The high fraction of poststarburst galaxies seen in our cluster sample is not mirrored in the surrounding field population and argues for an environmental mechanism for either the formation or prolonged visibility of this phase (D99).

The differences between cluster and field populations and the dynamic and spatial distributions of the "active" population (k + a/a + k and all emission classes) are consistent with these being recently acquired through infall from the field onto the clusters (D99), which in this scenario are responsible for transforming emission-line galaxies into k + a/a + k galaxies. If the "active" population is due to infall from the field, then given that the timescale of the k + a/a + k phase is about 1 Gyr, we can estimate the typical "survival time" of star formation as the ratio between the number of galaxies with emission lines and the number of k + a/a + k's. This timescale, τ_{em}, is about 1.5 Gyr and corresponds to the average time elapsed between the moment these galaxies "enter" the cluster (i.e., would be classified cluster members according to our criteria) and the moment they stop forming stars and therefore lose their emission lines. This corresponds to an average "infall rate" of 8–12 galaxies per Gyr per cluster, depending whether the k + a/a + k timescale is taken to be 1 or 1.5 Gyr. Assuming that the k + a/a + k population fades by a further magni-

TABLE 4

FRACTION OF GALAXIES AS A FUNCTION OF SPECTRAL CLASS

Cluster	k	k + a/a + k	e(a)	e(c)	e(b)	e	Number
Cl 1447+23	0.38 ± 0.13	0.06 ± 0.05	0.26 ± 0.10	0.26 ± 0.10	0.04 ± 0.04	0	21
Cl 0024+16	0.50 ± 0.07	0.14 ± 0.03	0.11 ± 0.03	0.18 ± 0.04	0.05 ± 0.02	0.02 ± 0.01	107
Cl 0939+47	0.46 ± 0.08	0.27 ± 0.06	0.09 ± 0.04	0.13 ± 0.04	0.03 ± 0.02	0.01 ± 0.01	71
Cl 0303+17	0.29 ± 0.07	0.16 ± 0.05	0.11 ± 0.05	0.23 ± 0.07	0.11 ± 0.05	0.10 ± 0.04	51
3C 295	0.53 ± 0.14	0.28 ± 0.10	0.07 ± 0.05	0.07 ± 0.05	0	0.04 ± 0.04	25
Cl 1601+42	0.59 ± 0.10	0.26 ± 0.07	0.07 ± 0.03	0.05 ± 0.03	0.03 ± 0.02	0	58
Cl 0016+16	0.55 ± 0.12	0.32 ± 0.09	0.08 ± 0.04	0.03 ± 0.03	0.03 ± 0.03	0	29
Total cluster	0.48 ± 0.04	0.21 ± 0.02	0.11 ± 0.02	0.14 ± 0.02	0.05 ± 0.01	0.02 ± 0.01	390
Field 0.35 < z < 0.60	0.30 ± 0.07	0.06 ± 0.03	0.11 ± 0.04	0.29 ± 0.06	0.16 ± 0.05	0.09 ± 0.03	71

TABLE 5

MEAN AND MEDIAN DISTURBANCE INDEX AS A FUNCTION OF THE
SPECTRAL CLASS

| | DISTURBANCE | | |
TYPE	Mean	Median	M/T/I/C/NULL[a]
k	0.36 ± 0.07	0.0 ± 0.0	1/7/9/0/47
k + a/a + k (red)	0.84 ± 0.22	1.0 ± 0.5	2/2/4/0/14
e(c)	1.00 ± 0.29	1.0 ± 0.6	0/1/4/1/6
k + a/a + k (blue)......	1.40 ± 0.39	1.0 ± 0.7	3/1/1/0/2
e(a)......................	1.47 ± 0.18	2.0 ± 0.5	4/4/0/0/12
e(b)	2.44 ± 0.29	2.0 ± 0.5	2/1/4/1/2

[a] M, merger; T, strong tidal interaction; I, weak tidal interaction; C, has a chaotic appearance; null, no interpretation listed in S97.

tude before entering the k class, this corresponds to about 12% of the cluster core luminosity acquired in the last Gyr.[15] Thus if, as expected in hierarchical models, the cluster has grown substantially in the recent past, this accretion has not consisted solely of star-forming field galaxies but is more likely to have been a mix of passive and star-forming galaxies.

If the presence of these star-forming galaxies in the clusters is related to the accretion of field galaxies, then their incidence is expected to depend on the infall rate (Bower 1991; Kauffman 1995a, 1995b; Tormen 1998) and the star-forming properties of galaxies in the field, both of which are likely to vary with redshift. The field population itself shows significant evolution with a large proportion of high-z field galaxies actively forming stars. In this scenario the Butcher-Oemler effect, defined as the *disappearance* of these star-forming galaxies at lower redshifts, is related to the cluster environment and its capability to halt star formation, which amplifies the trend of declining star formation at lower redshifts as compared with the field.

5.2. Morphological Properties
5.2.1. Morphology of the e(a) Population

In the previous section we noted that a common feature of the e(a) galaxies at low redshift is the evidence of mergers and/or strong interactions. From the morphological catalog (S97) it is possible to look for similar effects through what we have called the disturbance index (D) defined as 0: little or no asymmetry; 1 or 2: moderate or strong asymmetry; 3 or 4: moderate or strong distortion. The mean and median disturbance indices of each spectral class are shown in Table 5. The errors quoted are bootstrap estimates of the variances. The e(b) and e(a) distributions are significantly different from the k class and appear to be the most disturbed, but a χ^2 test shows that the difference in the mean D value between the e(a) and the e(c) class is not highly significant (50%).

We can also ask what the nature of the disturbance is in the e(a) and e(c) classes, using the visual interpretations of the nature of disturbance given in S97. These interpreta-

[15] We stress that this infall rate depends on the membership criteria adopted, which were chosen to minimize the field contamination and to ensure that any galaxy in the large-scale structure surrounding the clusters is retained (D99).

tions are based on whether the galaxy is an obvious merger (M), is undergoing a strong tidal interaction (T), a weaker tidal interaction (I), or has a chaotic appearance (C). We list in Table 5 the number of galaxies belonging to the M/T/I/C/null classes, where "null" means that no interpretation is listed in S97.

Using these classes we see a strong difference between the e(a) and e(c) populations, with all eight of the e(a) galaxies for which an interpretative class is listed being either mergers (4) or strong interactions (4), compared with only one of the six e(c)'s that are commented on [the remaining five e(c) galaxies show either weaker tidal features or a chaotic structure].

For the remaining e(a)'s and e(c)'s either no disturbance was found or no interpretation was given. Thus we suggest that at least a fraction of the e(a) galaxies are involved in a merger or strong tidal encounter. However, we also caution that it is difficult to assess the significance of their disturbance in a sample where large disk galaxies show in general a high incidence of nonaxisymmetric structure in comparison with their low-z counterparts (S97). To summarize, although e(a) galaxies are indistinguishable from e(c) galaxies in terms of frequency of disturbance compared with standard morphological forms, e(a)'s appear much more likely to be connected to mergers or strong interactions.

5.2.2. Passive Spirals

At low redshift there are numerous examples of spirals with weak or absent star formation, especially in clusters (see Koopmann & Kenney 1998 for a critical review of the correlation Hubble type to star formation activity in clusters; Kennicutt 1998 with references therein). Van den Bergh (1976) identified a class of "anemic" spirals having smooth arms that lack bright stars and H II regions that occur most frequently in clusters. These galaxies are deficient in neutral hydrogen but have normal CO emission (Kenney & Young 1986, 1989; van den Bergh 1991). The photometric properties of our k-type spirals are similar to those of the very red (yet H I–rich) spirals of types Sb and Sc from the sample of Schommer & Bothun (1983). These are luminous cluster spirals, but there are some field galaxies that share the same properties (NGC 1079, M31; see Schommer & Bothun for references), and it is not well established whether this phenomenon is more relevant in clusters. In the Schommer & Bothun sample some red spirals exhibit an anemic appearance, while others have a normal spiral structure with well-defined arms.

A systematic study of the kind carried out in D99 has not yet been undertaken for low-redshift clusters and therefore, although it is known that passive spirals are present in clusters both at low and high redshift, we cannot establish whether they are more/equally/less prevalent in low-z clusters than in distant ones. From our sample it is clear that at $z \sim 0.4$ the passive spirals are much more common in the clusters than in the field. In Figure 8 we compare the color distribution of the k-type cluster spirals with the distributions of other k-type Hubble types and the spirals with emission lines. The k-type spirals are *significantly redder* than the spirals with emission of similar Hubble type, and their color distribution is in fact intermediate between the E/S0's distribution and the spirals with emission. This confirms the reality of a separate population of "passive spirals" that cannot be due to "slit effects" (the slit missing
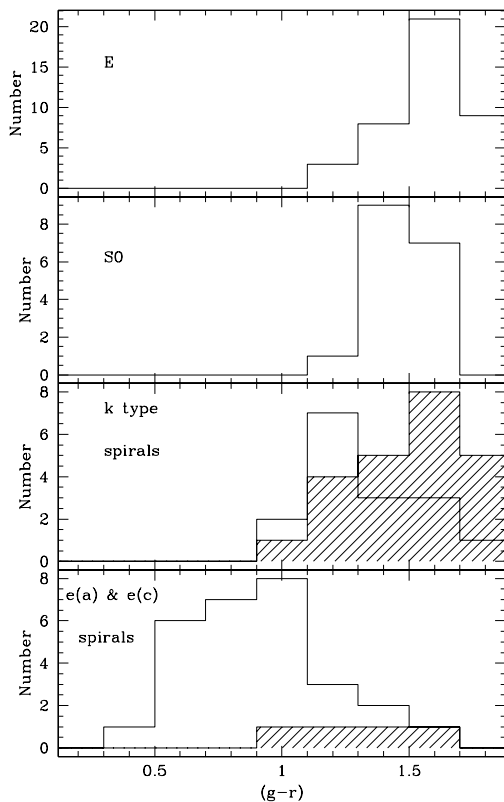
FIG. 8.—Color distributions of the k-type spirals as compared with other Hubble and spectral classes: k-type ellipticals (*top*); k-type S0's (*second panel from top*); k-type spirals of Sa type (*shaded area*) and Sb–later types (*empty histogram*; *third panel*); spirals with emission [e(a) and e(c) classes] of Sa's (*shaded area*) and Sb–later types (*empty histogram*) in the bottom panel.

a significant fraction of the disk light). Note that the difference in the color distribution between spirals with and without emission lines is not due to a higher fraction of early Sa galaxies, as this difference is still evident if one compares the distributions in the two bottom panels of Figure 8 separately for the Sa and the Sb–later types. We note that at present there is no evidence for a difference in the radial distributions of passive (k) and emission-line spirals, expected from the infall scenario, within the limited region imaged with *HST*.

It is reasonable to envisage the existence of an evolutionary connection between the k-type spirals and at least a fraction of the population of k + a/a + k galaxies with spiral morphologies, since it is obvious that the k-type spirals were forming stars at some point, and therefore they must have experienced a k + a/a + k phase during their evolution, soon after they stopped forming stars. However, the comparison of the number of k-type spirals (about 40 galaxies) with the number of k + a/a + k spirals (27 galaxies) suggests that—in the assumption of a k + a/a + k production constant in time—if the k + a/a + k spirals evolve into k types without changing morphology, they cannot retain their morphological characteristics for a time much longer than the k + a timescale, 1–1.5 Gyr.

The classification of a large proportion of the cluster spiral galaxies as k and k + a/a + k type suggests that the process responsible for halting star formation in these galaxies does not profoundly affect their morphology, at least

on a timescale comparable to the disappearance of the Balmer-strong signature. The prevalence of k and k + a/ a + k spirals in clusters points to an environmental process capable of stopping star formation (remove the gas reservoir) on a sufficiently short timescale to allow strong Balmer features to be visible for quite a long period. Moreover, the cessation of star formation must be achieved while retaining the broad morphological characteristics of the galaxy. The only process that the authors know of that acts exclusively on the gas content of the galaxy is stripping due to the intracluster medium.

Dressler et al. (1997) found that while the fraction of ellipticals in the clusters of this sample is comparable to that in low-redshift clusters, the fraction of S0 galaxies is 2–3 times lower than expected, with a corresponding increase in the spiral fraction. The k + a/a + k galaxies are the best candidates for S0 progenitors because of both their spectrophotometric characteristics and the predominance of disklike morphologies. The fact that the k + a/a + k galaxies are mostly spirals—i.e., *the spiral arms in their disks are still visible*—shows that the cessation of the star formation does not produce *at the same time* a change in morphology and that either two timescales or two different physical processes cause the two observed transformations, i.e., the halting of the star formation and the production of S0's. If this is the case, then the timescale of the "morphological evolution" (from spirals to S0's) must be longer than that of the spectrophotometric evolution (about 1 Gyr). The fact that S0's and ellipticals have indistinguishable color-magnitude relations in these distant clusters (Ellis et al. 1997) would be a natural consequence of this delayed morphological transformation. This issue will be discussed in detail in a forthcoming paper (Couch et al. 1999).

5.3. *Cluster-to-Cluster Variations*

Our sample includes clusters with a wide range in richness, mass, and X-ray luminosity (Smail et al. 1997a). We can therefore investigate the connection between star formation activity in the galaxy populations and the global cluster properties. Such connections could shed some light on the physical mechanism(s) responsible for the strong evolution in the galaxy populations within rich clusters between $z \sim 0.4$ and the present day.

We start by noting that all the clusters, except 3C 295, contain galaxies across the whole range of spectral classes (Table 4). The exception in 3C 295 is that there are no galaxies with e(b) spectra observed; however, this absence is not statistically significant. Overall the clusters show roughly comparable galaxy populations.

Although the spectral populations of the clusters show little variation, we wish to investigate whether the proportion of the active population of the clusters that are in a poststarburst phase correlates with any property of the cluster. The spectroscopic limit is similar in all the clusters, approximately $M_V = -19 + 5 \log_{10} h$ (D99), but it should be kept in mind that the level of completeness varies, and this could introduce some luminosity effects. X-ray luminosities, estimates of the central masses from lensing, and the integrated luminosity of the whole cluster galaxy population are available from Smail et al. (1997a) and the concentration index, C, and spiral fractions for the clusters from Dressler et al. (1997).

We compare the spectral properties of the centrally concentrated "regular" clusters (3C 295, Cl 0016+16, Cl

0024+16) with those of the less concentrated, irregular clusters (Cl 0303+17, Cl 0939+47, Cl 1447+23, Cl 1601+43). Interestingly, the spectral characteristics do not seem to depend on the dynamical state of the cluster. We analyze the proportion of galaxies with emission lines (em/all), the fraction of "active" galaxies act/all [where the active population is defined to include the following classes: k + a/a + k, e(a), e(c), e(b), e], and the proportion of k + a/a + k galaxies as a fraction of the total number of "active" galaxies (k + a, a + k/act); this latter quantity is a measure of the efficiency of environmental processes in stopping any star formation. No significant variation is found between the regular and the irregular clusters when divided in terms of their concentration. The ratio k + a, a + k/act is 0.41 ± 0.07 for the high-concentration clusters compared with 0.39 ± 0.06 for the low-concentration clusters. For em/all we find 0.29 ± 0.04 for high concentration and 0.34 ± 0.04 for low concentration, and for act/all we find 0.49 ± 0.05 versus 0.55 ± 0.05 for high- and low-concentration clusters, respectively. This result is especially interesting when compared with the conclusions of Dressler et al. (1997), who found in the centrally concentrated clusters a strong morphology–local galaxy density relation that is nearly absent in the irregular clusters. This again seems to suggest that the star formation histories and morphological properties may be separately affected by the clusters and in two different ways.

As regards the other global properties of the clusters (X-ray luminosities, masses, optical luminosities, spiral fractions), no definitive conclusion can be reached on the basis of their correlation with the proportion of the active population that is in a poststarburst phase. A larger sample of clusters with a range of properties (X-ray luminosities, masses, concentration indices) is needed in order to conclusively disentangle the mechanisms at work in producing the poststarburst population. We believe that such additional data, when combined with the kind of studies we have done in our relatively small sample, could be decisive in identifying the relevant mechanisms and processes.

6. CONCLUSIONS

By combining high-quality spectroscopic and morphological information on large samples of distant cluster and field galaxies we are finding evidence for two transformations of the cluster populations. The quicker and more striking transformation is associated with the widespread suppression of star formation in galaxies within the cluster environment. We have observed direct evidence for this process in the spectra of galaxies within our clusters, including populations of poststarburst (k + a/a + k) galaxies and passive (k) spirals. We further suggest that the bulk of the progenitors of the poststarburst population come from the emission-line galaxies with strong Balmer absorption [e(a)], which we interpret as dusty starbursts. We suggest that the active populations represent recently accreted field galaxies. Assuming that the mechanism that suppresses the star formation is prompt, this suggests that at least 12% of the luminosity of the cluster core has been acquired in the last 1 Gyr. The suppression process must act solely on the gas content of the galaxy without strongly affecting its morphological characteristics. We suggest that the process most likely to be responsible for the spectral evolution is ram-pressure stripping of the galaxy's gas supply by the cluster ICM. Gas exhaustion due to star formation and supernova-

driven winds are other possible mechanisms causing a dearth of interstellar medium that are expected to be at work in strong starbursts; since these processes are not directly connected with the cluster environment, it is difficult to understand why they would not produce a large k + a/a + k population also in the field, unless they act in combination with a cluster-related mechanism.

The second transformation—which appears to occur on a longer timescale—is harder to directly observe but is responsible for the formation of the dominant S0 population in local clusters, a group that is deficient in the distant clusters we have studied (Dressler et al. 1997). We suggest that this process is involved in the morphological conversion of the large populations of poststarburst and passive midtype spiral galaxies we see in these clusters. Whether this morphological transformation is a consequence of the same mechanism causing the quenching of star formation or whether another physical process is responsible for it (such as "galaxy harassment"; Moore et al. 1996, 1998) remains a fundamental question. Indeed, it is not obvious at this time whether any process other than passive fading of the disk light is needed to explain the morphological evolution of the disk galaxies.

Why should the infalling population be so evident at $z = 0.4$ and not at $z = 0$? The evolution in the field population surely plays a role: spectroscopic surveys of field galaxies have found that the star formation density is higher at $z = 0.4$ (Lilly et al. 1996; Ellis at al. 1996), i.e., more galaxies form stars more vigorously. The infall rate is also expected to increase at higher redshifts (Bower 1991; R. G. Bower 1998, private communication; Kauffmann 1995a, 1995b; Tormen 1998). Both of these effects will enhance the numbers of strongly star-forming galaxies encountering the cluster environment. When combined with possible evolution in the properties of the cluster ICM this may result in substantially more activity in the distant clusters.

We summarize the main conclusions of this work:

1. The class of cluster members with a very strong [O II] emission line [e(b), about 5% of the cluster sample] is mainly composed of low-luminosity, low-metallicity, late-type galaxies. They do not evolve into any other spectral class visible in our sample, and if their star formation is halted at some point, by $z = 0$ they will display the spectrophotometric properties of passive dwarfs.

2. Spectra with strong Balmer lines in absorption and [O II] in emission (about 10% of our cluster sample) cannot be reproduced by models with a regular, continuous star formation rate. A comparison with similar low-z spectra suggests that these are dusty galaxies whose star formation has been underestimated as a consequence of the extinction. These therefore are likely to be starburst galaxies and thus represent the best candidates for progenitors of the numerous poststarburst galaxies present in distant clusters. The low-z examples are associated with merging and strongly interacting galaxies; from the HST images of the distant clusters, a merger or strong interaction can clearly be associated with an e(a) spectrum in about half of the cases.

3. The main difference between the cluster and the field populations at $z \sim 0.4$–0.5 lies in the presence of a large number of poststarburst galaxies in the clusters (see the conclusions of D99). In contrast the population of dusty starbursts is numerous in both environments, although we have found possible weak evidence for an enhancement in the clusters. The differences between cluster and field are

consistent with a scenario in which the "active" galaxies (poststarburst and all emission-line galaxies) have been recently acquired by the clusters, whose most evident effect is the quenching of star formation. In the field the fraction of spirals with spectra similar to their low-z counterparts is higher than in the cluster (54%), with a considerable incidence of galaxies with enhanced star formation (24%).

4. Only 10% of the cluster members morphologically classified as spirals have spectra similar to low-redshift typical spirals, while the great majority have either an enhanced or suppressed star formation rate. We have identified a population of cluster spirals with "passive" spectra and red colors and discussed their probable association with at least a fraction of the poststarburst, spiral population. The fact that most of the poststarburst galaxies display spiral morphologies indicates that either the time-scale or the process responsible for halting the star formation must be different from the one that causes the morphological transformation. The passive spirals we observe could either subsequently evolve into passive S0's or preserve their morphological and spectrophotometric properties until $z = 0$. Detailed studies are needed to establish the incidence of passive spirals in low-z clusters.

5. A summary of results from all the aspects of the MORPHS program dealing with the evolution of the galaxy populations in distant clusters will be presented in Couch et al. (1999).

APPENDIX

METALLICITIES OF e(b) GALAXIES

There are various calibrations of the R_{23} index, based on direct measurements of the electron temperature for low-metallicity regions and photoionization models for high-metallicity regions. We adopt here the calibration given by Zaritsky, Kennicutt, & Huchra (1994), which is an average of three different calibrations:

$$12 + \log_{10} (\text{O/H}) = 9.265 - 0.33x - 0.202x^2 - 0.207x^3 - 0.333x^4 , \tag{A1}$$

where $x = \log_{10} (R_{23})$. The R_{23} index is especially valuable to estimate *relative* abundances, while the absolute calibration is more uncertain, typically 0.2 dex (Zaritsky et al. 1994).

The solar value is $[12 + \log_{10} (\text{O/H})] = 8.93$, $\log_{10} R_{23} \simeq 0.6$ according to equation (A1), and it is shown as a dotted line in Figure 9. H II regions in giant field spirals at low redshift have [O/H] between $+0.1$ and $+0.4$ solar, typically around $+0.3$ (Zaritsky et al. 1994), corresponding to a metallicity of 1.2–2.0 $Z/Z_\odot$.

The R_{23} index could be determined for 14 spectra out of the 20 e(b)-type cluster members in D99. For comparison purposes, we have also measured the index in the other spectral classes for any instances where the Hβ line was found in emission; this was possible in nine e(c), six color starburst (CSB)–e(c) [the bluest examples of e(c) galaxies; D99] and 17 e(a) spectra.

In our F_ν flux-calibrated spectra (see D99), we measured the line fluxes, applying a correction factor 1.753 to the [O II] flux to convert it into an F_λ flux relative to the [O III] and Hβ lines. In the case of the uncalibrated spectra in D99, the instrumental response as a function of λ was found from the comparison between the k-type spectra from D99 and an "elliptical" model (exponentially decaying SFR with a short timescale $\tau = 0.5$ Gyr) at each cluster redshift. The correction factor for the [O II] flux relative to [O III] was taken to be the ratio of the factors at the two observed wavelengths. This choice provides a lower limit for the [O II] flux and therefore an upper limit on the metallicities. A comparison between the index ranges of each given spectral type as derived from fluxed and uncalibrated spectra shows good agreement, confirming the validity of the correction applied to the uncalibrated spectra.

Before computing the index it is necessary to correct the observed Hβ flux for the underlying stellar absorption. The results shown in panel a of Figure 9 have been found applying a 5 Å correction or larger. The 5 Å value seems the most reasonable for the e(c) spectra, based on modeling of spiral spectra and the other observed Balmer lines in spirals. In Figure 9 the e(c) and the "CSB–e(c)" classes [very blue galaxies with an e(c) spectrum; D99] have been kept separated in order to study possible differences in metallicity. The e(a) spectra have by definition strong Balmer lines in absorption, and therefore in panel a we have chosen EW(Hβ)$_{\text{abs}}$ = EW(Hδ) if EW(Hδ) > 5 and EW(Hβ)$_{\text{abs}}$ = 5 Å otherwise. In the case of the e(b) spectra we
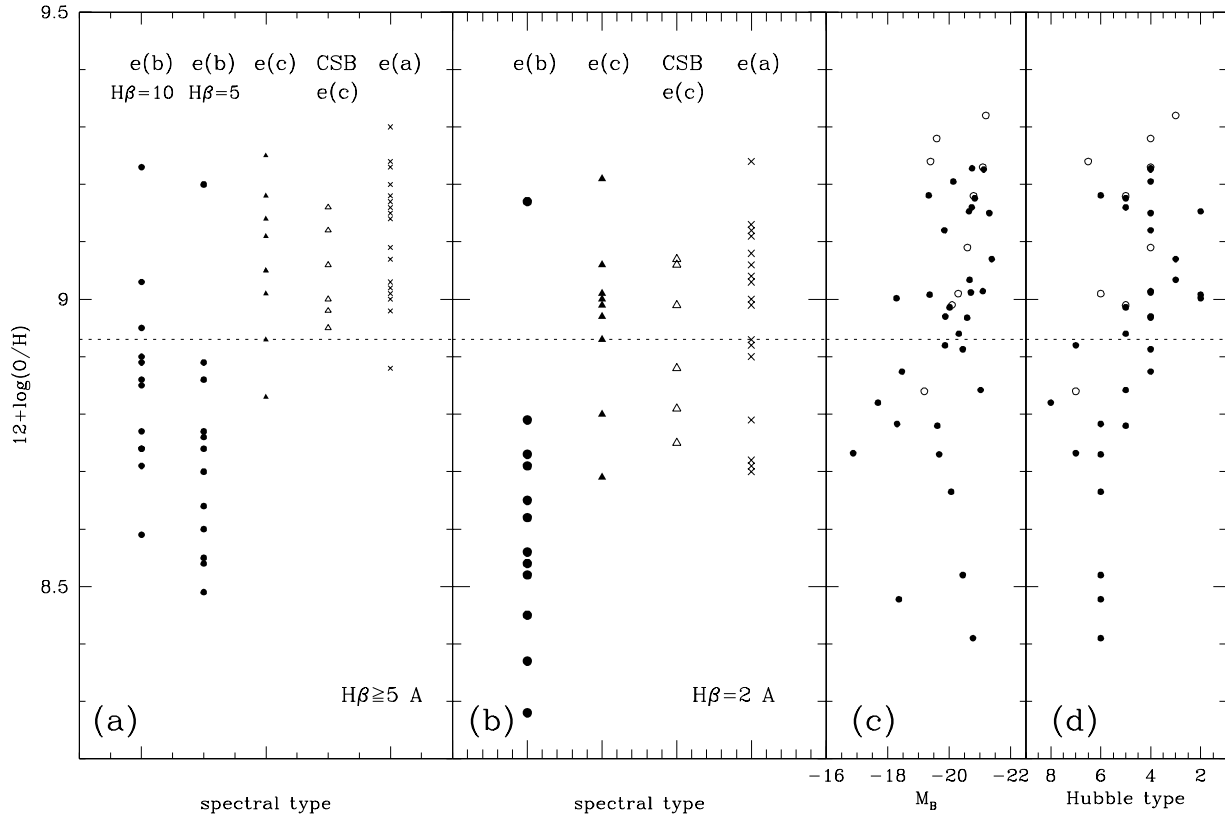
FIG. 9.—(a) and (b) show our distant cluster results as a function of the spectral type for different Hβ absorption corrections: (a) $H\beta_{abs} = 5$ Å, except in the case of e(b) ($H\beta_{abs} = 10$) and for the e(a) galaxies with $H\delta > 5$ Å ($H\beta_{abs} = H\delta$); (b) The adopted $H\beta_{abs}$ is 2 Å, the same as in (c) and (d). (c) and (d) show the data for low-redshift field spirals from Zaritsky et al. (filled dots) and Virgo spirals from Skillman et al. (1996; empty dots) as a function of the absolute B magnitude and of the T type. The plotted values are characteristic abundances measured at a given fraction of the isophotal radius ($0.4R_0$) and can be considered as representative of an "integrated abundance" (H. A. Kobulnicky 1998, private communication; Kobulnicky 1999; see also Kobulnicky & Zaritsky 1998). The data show that the mean abundance increases with the luminosity and for earlier Hubble types; this luminosity-metallicity relation is known to be valid to much fainter magnitudes, spanning over 10 magnitudes in M_B (not shown, see Zaritsky et al. 1994). Skillman et al. (1996) and previous works found that the most H I–deficient Virgo spirals have larger mean abundances than peripheral and field galaxies of comparable luminosity or Hubble type. Note that (c) and (d) cannot be directly compared with (a) because they have different $H\beta_{abs}$.

computed the index both for $H\beta_{abs} = 5$ and $H\beta_{abs} = 10$ Å, which is an appropriate limit for starburst galaxies (R. Terlevich 1998, private communication). Overestimating the correction for absorption (i.e., overestimating the Hβ flux in emission) results in an overestimate of the metallicities, and therefore the results in panel a can be regarded as upper limits on the absolute metal content.

The metallicities in e(b) H II regions are clearly lower than those in all the other emission spectral classes in our sample,[16] and this result is valid even for the most conservative choice of $H\beta_{abs}$ (10 Å). The H II regions in e(b) galaxies generally have lower than solar metallicity and display a wide range in Z (-0.5 dex solar to solar, $Z/Z_\odot$ between $\frac{1}{3}$ and 1, in the case $H\beta_{abs} = 5$ Å).

We next wish to compare the metallicities of our distant cluster galaxies with the data of nearby field and cluster spirals (Zaritsky et al. 1994; Skillmann et al. 1996; panels c and d in Fig. 9). The low-z spectra have been corrected with a fixed 2 Å $H\beta_{abs}$ and panel b of Figure 9 presents the metallicities of our sample found with the same correction. When comparing with the low-redshift data, one should bear in mind that the galaxies in our sample for which the Hβ line could be measured in emission (all galaxies in panels a and b of Fig. 9) belong to late Hubble types, typically Sbc or later (T types > 4); the e(b) subsample is mainly composed of Sd/Irr galaxies (T types 7–10; D99). We also notice that the spectra in our sample are not corrected for reddening, while the low-redshift spectra are, and our measures are therefore upper limits on the metallicities.

[16] While the R_{23} indexes (and therefore the metallicities) measured for the e(b) spectra can be considered as typical of this spectral class in our sample, it is uncertain whether the results for the e(c), CSB, and e(a) classes are representative of the whole sample of that given class: our spectra do not allow a reliable estimate of weak Hβ fluxes in emission, therefore we had to restrict this analysis to galaxies with a clear Hβ line in emission. These could represent the "most active" galaxies in each class and therefore probably the most metal-poor cases, if the usual metallicity–star formation relations are valid at this redshift. The sample is too small for a conclusive comparison between CSB and non-CSB e(c) spectra but suggests that the metallicities of the former class are more similar to those of the latter than to the e(b) galaxies. The relatively high z of CSB galaxies favors the hypothesis that the blue colors are due to strong star formation, as opposed to very low metallicities.

From Figure 9 we conclude that the H II region metallicities of the e(b) galaxies are significantly lower than those of any other spectral class and that these low abundances are comparable to those in low-luminosity, very late type spirals and the most luminous irregulars at low redshift.

REFERENCES

Abraham, R. G., et al. 1996, ApJ, 471, 694
Balogh, M. L., Morris, S. L., Yee, H. K. C., Carlberg, R. G., & Ellingson, E. 1997, ApJ, 488, L75
Balogh, M. L., Schade, D., Morris, S. L., Yee, H. K. C., Carlberg, R. G., Ellingson, E. 1998, ApJ, submitted (astro-ph 9806146)
Barbaro, G., & Poggianti, B. M. 1997, A&A, 490, 504
Barger, A. J., Aragon-Salamanca, A., Ellis, R. S., Couch, W. J., Smail, I., & Sharples, R. M. 1996, MNRAS, 279, 1
Barger, A. J., et al. 1998, ApJ, 501, 522
Belloni, P., Bruzual, A. G., Thimm, G. J., & Roser, H.-J. 1995, A&A, 297, 61
Bower, R. G. 1991, MNRAS, 248, 332
Bower, R. G., Lucey, J. R., & Ellis, R. S. 1992, MNRAS, 254, 601
Butcher, H., & Oemler, A., Jr. 1978, ApJ, 226, 559
———. 1984, ApJ, 285, 426
Byrd, G., & Valtonen, M. 1990, ApJ, 350, 89
Carter, D., Prieur, J. L., Wilkinson, A., Sparks, W. B., & Malin, D. F. 1988, MNRAS, 235, 813
Couch, W. J., Barger, A. J., Smail, I., Ellis, R. S., & Sharples, R. M. 1998, ApJ, 497, 188
Couch, W. J., et al. 1999, in preparation
Couch, W. J., Ellis, R. S., Sharples, R. M., & Smail, I. 1994, ApJ, 430, 121
Couch, W. J., & Sharples, R. M. 1987, MNRAS, 229, 423 (CS87)
Dressler, A., et al. 1997, ApJ, 490, 577
Dressler, A., & Gunn, J. E. 1982, ApJ, 263, 533
———. 1983, ApJ, 270, 7
———. 1992, ApJS, 78, 1
Dressler, A., Oemler, A., Jr., Butcher, H., & Gunn, J. E. 1994, ApJ, 430, 107
Dressler, A., Smail, I., Poggianti, B. M., Butcher, H., Couch, W. J., Ellis, R. S., & Oemler, A., Jr. 1999, ApJS, 122, in press (D99)
Duc, P. A., Mirabel, I. F., & Maza, J. 1997, A&AS, 124, 533
Edmunds, M. G., & Pagel, B. E. J. 1984, MNRAS, 211, 507
Ellis, R. S., Colless, M., Broadhurst, T. J., Heyl, J. S., & Glazebrook, K. 1996, MNRAS, 280, 235
Ellis, R. S., Smail, I., Dressler, A., Couch, W. J., Oemler, A., Jr., Butcher, H., & Sharples, R. M. 1997, ApJ, 483, 582
Fabricant, D. G., Bautz, M. W., & McClintock, J. E. 1994, ApJ, 107, 8
Fabricant, D. G., McClintock, J. E., & Bautz, M. W. 1991, ApJ, 381, 33
Fisher, D., Fabricant, D., Franx, M., & van Dokkum, P. 1998, ApJ, 498, 195
Gallego, J., Zamorano, J., Rego, M., & Vitores, A. G. 1997, ApJ, 475, 502
Gunn, J. E., & Gott, J. R. 1972, ApJ, 176, 1
Hammer, F., et al. 1997, ApJ, 481, 49
Hammer, F., & Flores, H. 1998, preprint (astro-ph 9806184)
Henry, J. P., & Lavery, R. J. 1987, ApJ, 323, 473
Jacoby, G. H., Hunter, D. A., & Christian, C. A. 1984, ApJS, 56, 257
Kauffmann, G. 1995a, MNRAS, 274, 153
———. 1995b, MNRAS, 274, 161
Kenney, J. D. P., & Young, J. S. 1986, ApJ, 301, L13
———. 1989, ApJ, 344, 171
Kennicutt, R. C., Jr. 1992a, ApJS, 79, 255
———. 1992b, ApJ, 388, 310
———. 1998, ARA&A, 36, in press

Kim, D. C., Veilleux, S., & Sanders, D. B. 1998, ApJ, 508, 627
Kobulnicky, H. A. 1999, in preparation
Kobulnicky, H. A., & Zaritsky, D. 1998, in preparation
Koo, D. C., Guzmán, R., Gallego, J., & Wirth, G. D. 1997, ApJ, 478, L49
Koopmann, R. A., & Kenney, J. D. P. 1998, ApJ, 497, L75
Kurucz, R. L. 1993, CD-ROM 13, ATLAS9 Stellar Atmosphere Programs and 2 km/s Grid (Cambridge: Smithsonian Astrophys. Obs.)
Lavery, R. J., & Henry, J. P. 1986, ApJ, 304, L5
———. 1988, ApJ, 330, 596
Lilly, S. J., LeFevre, O., Hammer, F., & Crampton, D. 1996, ApJ, 460, L1
Liu, C. T., & Kennicutt, R. C., Jr. 1995a, ApJS, 100, 325
———. 1995b, ApJ, 450, 547
Moore, B., Katz, N., Lake, G., Dressler, A., & Oemler, A., Jr. 1996, Nature, 379, 613
Moore, B., Lake, G., & Katz, N. 1998, ApJ, 495, 139
Morris, S. L., Hutchings, J. B., Carlberg, R. G., Yee, H. K. C., Ellingson, E., Balogh, M. L., Abraham, R. G., & Smecker-Hane, T. A. 1998, preprint (astro-ph 9805216)
Newberry, M. V., Boroson, T. A., & Kirshner, R. P. 1990, ApJ, 350, 585
Oemler, A., Jr., Dressler, A., & Butcher, H. 1997, ApJ, 474, 561
Osterbrock, D. E. 1989, Astrophysics of Gaseous Nebulae and Active Galactic Nuclei (Mill Valley: Univ. Sci.)
Pagel, B. E. J., Edmunds, M. G., Blackwell, D. E., Chun, M. S., & Smith, G. 1979, MNRAS, 189, 569
Poggianti, B. M. 1994, Ph.D. thesis, Univ. Padova
Poggianti, B. M., & Barbaro, G. 1996, A&A, 314, 379
———. 1997, A&A, 325, 1025
Poggianti, B. M., & Wu, H. 1999, in preparation
Sandage, A. 1986, A&A, 161, 89
Sanders, D. B., & Mirabel, I. F. 1996, ARA&A, 34, 749
Schommer, R. A., & Bothun, G. D. 1983, ApJ, 88, 577
Skillman, E. D., Kennicutt, R. C., Jr., Shields, G. A., & Zaritsky, D. 1996, ApJ, 462, 147
Smail, I., Dressler, A., Couch, W. J., Ellis, R. S., Oemler, A., Jr., Butcher, H., & Sharples, R. M. 1997b, ApJS, 110, 213 (S97)
Smail, I., Ellis, R. S., Dressler, A., Couch, W. J., Oemler, A., Jr., Butcher, H., & Sharples, R. M. 1997a, ApJ, 479, 70
Smail, I., Ivison, R. J., Blain, A. W., & Kneib, J.-P. 1998, ApJ, 507, L21
Soucail, G., Mellier, Y., Fort, B., & Cailloux, M. 1988, A&AS, 73, 471
Stasinska, G. 1990, A&AS, 83, 501
Tormen, G. 1998, MNRAS, 297, 648
van den Bergh, S. 1976, ApJ, 206, 883
———. 1991, PASP, 103, 390
van Dokkum, P. G., & Franx, M. 1996, MNRAS, 281, 985
van Dokkum, P. G., Franx, M., Kelson, D. D., Illingworth, G. D., Fisher, D., & Fabricant, D. 1998, ApJ, 500, 714
Wilson, G., Smail, I., Ellis, R. S., & Couch, W. J. 1997, MNRAS, 284, 915
Wirth, G. D., Koo, D. C., & Kron, R. G. 1994, ApJ, 435, L105
Wu, H., Zou, Z. L., Xia, X. Y., & Deng, Z. G. 1998, A&A, in press
Zabludoff, A. I., Zaritsky, D., Lin, H., Tucker, D., Hashimoto, Y., Shectman, S. A., Oemler, A., & Kirshner, R. P. 1996, ApJ, 466, 104
Zaritsky, D., Kennicutt, R. C., Jr., & Huchra, J. P. 1994, ApJ, 420, 87